Copy No._____

Defence Research and Development Canada
Recherche et développement pour la défense Canada

DEFENCE R&D DÉFENSE

# An Evaluation of Side-Looking 12 and 100 kHz Sonars for Continuous Surveillance of a Shallow Channel

*Mark V. Trevorrow*

**Defence R&D Canada**

Technical Memorandum
DRDC Atlantic TM 2002-149
September 2002

Canada

# An Evaluation of Side-Looking 12 and 100 kHz Sonars for Continuous Surveillance of a Shallow Channel

Mark V. Trevorrow

**Defence Research and Development Canada – Atlantic**

Technical Memorandum

DRDC Atlantic TM 2002-149

September 2002

106-03680/

Author

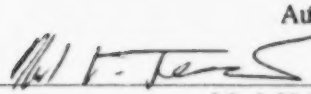

Mark V. Trevorrow

Approved by

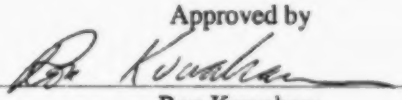

Ron Kuwahara

Head, Signatures Section

Approved for release by

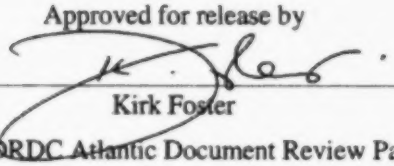

Kirk Foster

Chair, DRDC Atlantic Document Review Panel

© Her Majesty the Queen as represented by the Minister of National Defence, 2002

© Sa majesté la reine, représentée par le ministre de la Défense nationale, 2002

## Abstract

This study evaluates data from two high-frequency (12 and 100 kHz) side-looking sonars which were operated for extended periods in March and October 1997 in Drogden Channel, near Copenhagen, Denmark. This busy shipping channel, 1-km-wide by 12-m-deep, connects the Baltic Sea with the North Sea through the Kattegat. The original purpose of these tests was to demonstrate continuous surveillance for migratory herring, however a variety of shipping traffic was also observed. Quantitative acoustic measurements of ship characteristics and low-grazing-angle seabed reverberation were made with both sonars under a variety of conditions. The sonar measurements were supplemented by simultaneous water temperature, salinity, and current profiles and surface meteorological measurements, allowing some understanding of the environmental influences. The general characteristics were that under normal, homogeneous flow conditions, ships and fish schools were routinely observed up to 400 m range with the 100 kHz sonar and up to 2000 m range with the 12 kHz system. Occasional saline intrusions near the seabed were observed to create strong upward-refracting conditions that significantly altered the available range for target detection, especially for the 100 kHz sonar. Example echograms and reverberation results from both normal and upward-refracting conditions are shown. Ray-tracing analysis is used to assess the acoustic propagation conditions, specifically to define insonified volumes and shadow zones, and quantify the reflection focusing effects.



## Résumé

Cette étude évalue les données provenant de deux sonars haute fréquence (12 et 100 kHz) à balayage latéral qui ont été utilisés durant de longues périodes en mars et en octobre 1997 sur le canal de Drogden, près de Copenhague au Danemark. Ce canal de navigation achalandé, d'une largeur de 1 km et d'une profondeur de 12 m, relie la mer Baltique à la mer du Nord par le Kattegat. Les essais, qui visaient initialement à faire la démonstration d'une surveillance continue du hareng migrateur, ont toutefois servi également à observer le trafic maritime. On a effectué des mesures acoustiques quantitatives des caractéristiques des navires et de la réverbération du fond marin aux faibles angles d'incidence, à l'aide des deux sonars et dans diverses conditions. Les mesures des sonars ont simultanément été complétées par des relevés de température et de salinité de l'eau, par des profils de courants et par des mesures météorologiques en surface, qui ont permis de comprendre un peu mieux les influences de l'environnement. Dans des conditions normales d'écoulement homogène, on a généralement pu observer des navires et des bancs de poissons jusqu'à une distance de 400 m avec le sonar de 100 kHz et jusqu'à une distance de 2 000 m avec le sonar de 12 kHz. Il s'est avéré que des marées salines occasionnelles près du fond marin créaient des conditions de forte réfraction vers le haut qui réduisaient considérablement la distance de détection possible des cibles, surtout dans le cas du sonar de 100 kHz. Des exemples d'échogrammes et de résultats de réverbération dans des conditions normales et de réfraction vers le haut sont présentés. Une analyse de tracé de rayon permet d'évaluer les conditions de propagation acoustique dans le

but précis de définir les volumes insonifiés et les zones d'ombre ainsi que de quantifier les effets de concentration des réflexions.

# Executive summary

**Introduction**

These 12 and 100 kHz sonar data were collected through 1996-98 as part of an international environmental monitoring program, and have been recently re-examined to assess the feasibility of high-frequency sonar for underwater surveillance against targets such as AUVs, torpedoes, and SCUBA divers. The simultaneous collection of ancillary oceanographic data allows assessment of the impacts of changing water flow and surface meteorological conditions on sonar performance.

**Principal Results**

The data show detection characteristics of a variety of ships, up to 400 m range with the 100 kHz sonar and up to 2000 m range with the 12 kHz system, in this 10 to 13 m depth channel. The dominant limitation was relatively high-levels of boundary reverberation, both from the seabed and surface. Quantitative measurements of acoustic reverberation under a variety of conditions were made with both sonars. Subtle changes in water stratification strongly altered the acoustic propagation conditions, in most cases drastically degrading sonar performance, especially for the vertically narrow-beam 100 kHz sonar.

**Significance of the Results**

The sonar data on vessel detectability and the signal to reverberation ratios under a variety of flow conditions are a useful demonstration of the feasibility and limitations of high-frequency sonar for underwater surveillance. These results will serve as benchmark in any future design study. The limitations imposed by boundary reverberation imply that site selection is highly important for the success of a sonar surveillance operation. The drastic impact of changes in flow conditions suggests that i) continuous oceanographic measurements must be made alongside the surveillance sonar, and ii) acoustic propagation analyses should be performed to assess the impact of changes in water properties.

**Future Plans**

It is recommended that a series of measurements focused on verifying narrow-beam sonar detectability concepts on AUVs and SCUBA divers be performed in a variety of well-characterized shallow water environments. Also, there is a need for high-resolution acoustic target strength measurements as a function of frequency and incidence angle for targets of naval interest (e.g. torpedoes, AUVs, and scuba divers).

Trevorrow, M., 2002. An Evaluation of Side-Looking 12 and 100 kHz Sonars for Continuous Surveillance of a Shallow Channel. TM 2002-149. DRDC Atlantic.

# Sommaire


## Introduction

Dans le but d'évaluer la faisabilité du sonar haute fréquence pour la surveillance sous-marine de cibles comme des véhicules sous-marins autonomes (AUV), des torpilles et des plongeurs autonomes, on a récemment réexaminé des données de sonars de 12 et de 100 kHz recueillies de 1996 à 1998 dans le cadre d'un programme international de surveillance de l'environnement. La collecte simultanée de données océanographiques auxiliaires permet d'évaluer l'impact des variations de l'écoulement d'eau et des conditions météorologiques de surface sur les performances des sonars.

## Principaux résultats

Les données montrent les caractéristiques de détection de différents navires, jusqu'à une distance de 400 m pour le sonar de 100 kHz et jusqu'à une distance de 2 000 m pour le sonar de 12 kHz, dans le canal d'une profondeur de 10 à 13 m. Les principales restrictions tiennent aux niveaux relativement élevés de réverbération par les couches limites, tant sur le fond marin qu'en surface. On a effectué des mesures quantitatives de la réverbération acoustique dans diverses conditions, à l'aide des deux sonars. Les légères variations de la stratification de l'eau ont fortement altéré les conditions de propagation acoustique, ce qui, dans la plupart des cas, a nettement dégradé les performances des sonars, surtout pour ce qui est du sonar de 100 kHz à faisceau étroit vertical.

## Importance des résultats

Les données des sonars sur les possibilités de détection des navires et sur les rapports signal/réverbération dans diverses conditions d'écoulement constituent une démonstration utile de la faisabilité et des restrictions du sonar haute fréquence pour la surveillance sous-marine. Les résultats serviront de points de référence pour toute étude future de conception. Les restrictions qu'impose la réverbération par les couches limites impliquent que la sélection des emplacements revêt une grande importance pour la réussite des opérations de surveillance par sonar. L'impact marqué des variations des conditions d'écoulement révèle i) que les mesures océanographiques continues doivent être effectuées en mêmetemps at au même endroit que le sonar de surveillance et ii) que des analyses de propagation acoustique devraient être effectuées dans le but d'évaluer l'impact des variations des propriétés de l'eau.

## Plans pour l'avenir

On recommande de consacrer une série de mesures aux possibilités de détection des AUV et des plongeurs autonomes à l'aide d'un sonar à faisceau étroit, dans divers environnements bien caractérisés en eaux peu profondes. Il est également nécessaire de mesurer l'intensité des cibles acoustiques à haute résolution en fonction de la fréquence et de l'angle d'incidence dans le cas des cibles d'intérêt militaire (p. ex. torpilles, AUV et plongeurs autonomes).

Trevorrow, M., 2002. An Evaluation of Side-Looking 12 and 100 kHz Sonars for Continuous Surveillance of a Shallow Channel. TM 2002-149. RDDC Atlantic.

## Acknowledgments

The original field work through 1996-98 was supported by the Danish Environmental Protection Agency, Kontroll- och Styrgruppen för Öresundsforbindelsen (KSÖ Sweden) and Øresundskonsortiet A/S. The author is indebted to Dr. Bjarke Pedersen of LICEngineering A/S (Denmark) for his efforts throughout 1996-98 in installing and maintaining the sonar system during these collaborative field trials. Overall project leadership was provided by Drs. David Farmer of the Institute of Ocean Sciences (Sidney, B.C.) and Niels-Eric Ottesen-Hansen of LICEngineering A/S (Hellerup, Denmark).

# Table of contents

Abstract ..... i

Résumé ..... i

Executive summary ..... iii

Sommaire ..... iv

Acknowledgments ..... vi

Table of contents ..... vii

List of Figures: ..... viii

1. Introduction ..... 1

2. Description of Site and Instrumentation ..... 5

3. 100 kHz Reverberation and Target Detection Results ..... 10

4. 12 kHz Reverberation and Target Detection Results ..... 17

5. Propagation Modeling ..... 21

6. Concluding Discussions and Recommendations ..... 24

7. Bibliography ..... 27

# List of Figures:

Figure 1 Left: map of the Øresund and NW Baltic showing the sonar installation site in Drogden Channel. Right: 2002 photograph of new Oresund link bridge looking westward from Malmo towards Drogden Channel, with Amager and Copenhagen in far background. ..... 5

Figure 2 Photograph of the 12 kHz sonar array mounted on a tripod with stepping motor, prior to deployment in Drogden Channel, Denmark in early October, 1997. ..... 6

Figure 3 Comparison of near-surface (2.9 m depth, black) and near-bottom (9 m depth, red) temperature, salinity, and along-channel (North) current at mid-water depth (near 4.8 m depth) in Drogden Channel during March 1997. ..... 8

Figure 4 Comparison of near-surface (2.9 m depth, black) and near-bottom (9 m depth, red) temperature, salinity, and sound speed in Drogden Channel during October 1997. ..... 9

Figure 5 Wind speed and direction for March 1997 at Drogden Channel, Denmark. ..... 9

Figure 6 100 kHz cross-channel *ETS* (dB re 1 $m^2$) vs. range and time starting 1328UT March 16th, 1997. Labels S indicate ships and TC the echo from temperature-conductivity sensor mooring. ..... 10

Figure 7 Seabed reverberation vs. range profile averaged over 20 minutes starting 1444UT, March 16, 1997. Compared to simple seabed scattering model using constant $S_A$ = -30 dB. ..... 11

Figure 8 100 kHz cross-channel *ETS* (dB re 1 $m^2$) vs. range vs. time starting 0106UT March 15th, 1997. Regions of seabed and surface reverberation are indicated, with labels S indicating ships, TC the echo from temperature-conductivity mooring, and ADCP the echo from a surface float at that location. ..... 12

Figure 9 Comparison of seabed and surface dominated reverberation levels vs. range at 100 kHz, averaged over 10-minute intervals before and after the transition event at 0300UT March 15$^{th}$, 1997. ..... 12

Figure 10 Comparison of reverberation during periods of light (4 m/s) and strong (16 m/s) surface winds under normal flow conditions, March 18, 1997. ..... 13

Figure 11 Comparison of reverberation during periods of light (3.6 m/s) and strong (10.3 m/s) surface winds under saline intrusion flow conditions, March 15, 1997. ..... 13

Figure 12 Example ship wake signature at 0500UT March 22, 1997. Ship speed (from hyperbolic trajectory) was 3.2 m/s with maximum *ETS* (at closest approach) of -0.4 dB (re 1 $m^2$). ..... 14

Figure 13 Comparison of ship hull *ETS* (dB re 1 $m^2$) with background reverberation (0114UT March 15) under normal flow conditions. A total of 593 ship targets were observed from March 14 to 31. ..... 15

Figure 14 Distribution of measured ship speeds extracted from hyperbolic trajectory fitting of sonar signatures from March 14-31, 1997 in Drogden Channel. ..... 16

Figure 15 Fixed orientation 12 kHz *ETS* (dB re 1 $m^2$) vs. range and time starting 1428UTC Oct. 14, 1997 in Drogden Channel. ..... 17

Figure 16 Comparison of ship's hull *ETS* with background reverberation for the fixed-orientation 12 kHz sonar in Drogden Channel, Oct 14, 1997. Reverberation curve averaged over 1890 pings starting 1332UTC. Ship's hull data taken from 58 ships observed over entire 0500-1838h period..... 18

Figure 17 12 kHz sector scan image in *ETS* (dB re 1 $m^2$) showing background reverberation and two ship signatures, taken 1224UTC Oct. 29, 1997 in Drogden Channel. Image was constructed from 26 pings covering a 50° by 1800m sector, requiring 150 s to complete.19

Figure 18 Comparison of ship's hull *ETS* with background reverberation for the sector scanning 12 kHz sonar in Drogden Channel, Oct 29/30, 1997. Reverberation curves were averaged over 1960 pings at all azimuthal angles. Ship's hull *ETS* taken from 95 ships observed over the entire 28-hour period. ..... 20

Figure 19 Comparison of ray-tracing predictions of normalized sound pressure level (one-way transmission loss + 20log[r]) vs. range and depth for the 100 kHz sonar in Drogden Channel. Rays launched ±3.5° from horizontal. (a) normal flow regime. (b) saline intrusion regime..... 22

Figure 20 Comparison of ray-tracing predictions of normalized sound pressure level (one-way transmission loss + 20log[r]) vs. range and depth for the 120 kHz sonar in Drogden Channel. Rays launched ±20° from horizontal. (a) normal flow regime. (b) saline intrusion regime..... 23

# 1. Introduction

Side-looking, high-frequency active sonars offer a promising approach for continuous surveillance of harbours and strategic waterways. The purpose of such surveillance might be to quantify migration of fish or marine mammals, or in a defense or security scenario for the detection of small boats, autonomous underwater vehicles (AUVs), torpedoes, or SCUBA divers. Fixed side-looking sonar installations offer the capability for continuous, full-water-depth surveillance at ranges of 100's to 1000's of meters. In relatively noisy underwater environments where covert operation is not required, such as harbours or in the vicinity of anchored surface vessels, active sonars offer improved detectability over passive systems. Furthermore, since the ocean is largely opaque to radar and laser systems, particularly in turbid coastal or estuarine situations, acoustics is often the only alternative for remote detection of small underwater targets. However, the ability to probe close to the boundaries in stratified, shallow-water environments is strongly limited by both reverberative interference and acoustic propagation effects. Reverberation from the surface and seabed masks the echoes from smaller targets, in essence creating a range and time-dependent detection threshold. The effects of acoustic propagation, namely the focusing and shadow zones created by boundary reflections and internal refraction, are to create non-uniform detection volumes and to modify the boundary reverberation levels.

Many of these limitations have been encountered in previous studies on the detection of fish (and other targets) using similar side-looking sonars. Beginning in the 1960's work reported by Weston, Revie, and others (1971, 1989, 1990) demonstrated long-range (up to 65 km) sonar concepts, including detection of fish schools, using a high-power military sonar installation near Perranporth, England. More recently the use of short-range (<100 m) side-looking sonars for fish detection in rivers and lakes has been gaining acceptance. For example, a recent study by the author (Trevorrow 1997) showed that adult salmon (60 cm length) can be detected in a shallow riverine environment at ranges up to 200 to 300 m, depending on reverberation conditions. These earlier studies with fish suggest that larger acoustic targets, such as AUVs or divers, should be detectable at useful ranges (of order 100's to 1000's of meters) with appropriately designed high-frequency sonars and an understanding of the acoustic reverberation and propagation environment.

The purpose of this present work is to examine the reverberation levels and target detectability during field evaluations of two distinct side-looking sonars, one operating at 12 kHz and the other at 100 kHz. These sonar installations were deployed and operated for extended periods during 1996-98 in Drogden Channel, Denmark, as part of an environmental monitoring program during the construction of a bridge and tunnel connecting Copenhagen, Denmark and Malmö, Sweden. This shallow channel (<14 m deep) is a busy shipping lane connecting the Baltic Sea with the Kattegat, and thus is a realistic location for operation of a surveillance sonar. This location also provided a large number of *ships of opportunity* of various sizes for use as test targets. The original purpose of these sonar deployments was the monitoring of migratory herring, as described by two earlier papers (Pedersen & Trevorrow 1999; Farmer et al. 1999). An important aspect of this project was that the sonars were operated continuously over extended periods, allowing investigation of the effects of temporal changes in water properties. Surface weather and water temperature, salinity, and current profiles were monitored continuously alongside the sonar installation. This allows a quantitative investigation of the environmental influences on acoustic propagation and reverberation. An

abbreviated version of this work was presented by the author at a SACLANTCEN conference on littoral environmental variability in Sept. 2002.

Before proceeding with analysis of the field data, it is useful to review the expected echo strength of the various targets of interest in a typical underwater surveillance operation. Target Strength (*TS*) in deciBels (dB) is defined as 10 times the common logarithm of the *backscatter cross-section* in $m^2$, which is equivalent to the ratio of reflected to incident acoustic intensity for an object. In the simplest model for mid- to high-frequency sonars operating on relatively large objects, i.e. in a regime where the acoustic wavelength is much smaller than the object size, the *total* scattering cross-section approaches the *geometric* incidence area. In this regime it is common to convert *total* to *backscatter* cross-section by dividing by $4\pi$, which is strictly valid only for isotropic scatterers. For larger complex targets, the scattering cross-section will be strongly moderated by internal resonances and is strongly dependent on aspect angle in the case of elongated objects (e.g. cylinders). Predicting the exact scattering cross-section is theoretically and computationally difficult, however a useful simplification is to identify rigid or air-filled components of the target, e.g. the lungs of a marine mammal or the cylindrical air tanks of a SCUBA diver. Because of the strong contrast in acoustic impedance between water and air or metal, acoustic scattering will be dominated by these sub-components. Thus, for performance modeling purposes acoustic scattering models for these simple objects can be used to produce rough (± 3 dB) *TS* estimates for these specific targets. In future these *TS* estimates need to be confirmed and refined with field measurements.

The simplest scatterer is a rigid or air-filled sphere, whereby the high-frequency (wavelength << radius) *total* scattering cross-section approaches the incidence area $\pi a^2$, where $a$ is the radius (see Medwin and Clay 1998; Stanton 1989). Then the sphere $TS = 10 \log_{10}[a^2 / 4]$. This relation is in close agreement with measurements reported by Cotaras (1991). For cylindrical targets the scattering is more complicated, being generally composed of a *background* omni-directional scattering with strong *highlights* at broadside and end aspect. The *background* cross-section is given with reasonably accuracy by one-half the geometric cross-section at broadside incidence, i.e. the product of $a$ and $L$, the cylinder radius and length. Then the background *TS* can be given by $10 \log_{10}[a L / 4\pi]$. For example with a 28 cm diameter by 91 cm long air-filled cylinder, the predicted background *TS* is –20 dB (re 1 $m^2$), very close to values measured at 33 kHz by Cotaras (1991). The broadside highlight from a cylinder is similar in form to that of a line-array of sources (see Medwin and Clay 1998; Stanton 1989; Chapman 1991), i.e.

$$\sigma_{total} = k \cdot a \cdot L^2 \cdot [\sin(\beta) / \beta]^2 \cdot \cos^2 \theta, \qquad \beta = k \cdot L \cdot \sin\theta$$

where $k$ is the acoustic wavenumber ($m^{-1}$) and $\theta$ is the incidence angle (0 at broadside). For this broadside highlight the strength increases and width decreases with increasing frequency. At exactly broadside incidence the *TS* reduces to $10 \log_{10}[a L^2 / 2 \lambda]$, where $\lambda$ is the acoustic wavelength. Similarly for the end-aspect highlight (assuming flat end-caps), the scattering is similar to that from a circular disk, with expected on-axis $TS = 20 \log_{10}[\pi a^2 / \lambda]$. Measurements by Cotaras (1991) clearly show these highlights, e.g. for the same 28 x 91 cm air-filled cylinder at 33 kHz the broadside and end-aspect highlights were –6 ± 1 dB and –2 ± 2 dB, respectively (as compared to the –20 dB background). However, these measured highlights were both roughly 7 dB below the predictions, presumably a result of the cylinder not being a perfectly rigid, lossless reflector. It is tempting to apply this highlight correction factor to predicted *TS* estimates, however this will be dependent on the detailed internal

structure of the object and it is inadvisable to generalize. The measured angular widths of the highlights, typically 1° - 2° at 30 kHz, were in agreement with the above formulae. A similar formula for the broadside highlight from a prolate spheroid is given by Stanton (1989).

**Table 1:** Summary of measured and predicted *TS* values for various surveillance sonar targets. BS = broadside incidence, E = end incidence, BG = background (omni-directional). All *TS* in dB re 1 $m^2$. No corrections for acoustic penetrability were made to the BS and E highlight predictions, which thus might be overestimates. Acoustic highlights from cylinders are typically 1° to 2° wide.

| Target Type | Model/Size | TS 12kHz | TS 100kHz | Comments |
|---|---|---|---|---|
| Adult salmon | 60 cm empirical | -25 dB BS | -28 dB BS | see Love (1977) and Dahl & Mathisen (1983) |
| Herring (*Clupea harangus*) school | measured | -20 dB | -14 dB | see Pedersen & Trevorrow (1999) and Farmer et al. (1999). |
| Dolphin (*Tursiops truncatus*) | measured: 2.2 m length, 126 kg | -11 dB BS<br>-16 dB head<br>-32 dB tail | -20 dB BS<br>-25 dB head<br>-40 dB tail | see Au (1996) |
| Humpback whale (*Megaptera novaeangliae*) | measured at 20 kHz, 15m long | +7 dB BS<br>-4 dB head | +2 dB BS<br>-9 dB head | see Love (1973) |
| Right whale (*Eubalaena glacialis*) | measured at 86 kHz, 13-15m long | +3 dB BS<br>-7 dB head | -2 dB BS<br>-12 dB head | see Miller & Potter (2001) |
| mid-water mine | sphere, 1 m diameter | -12 dB | -12 dB | neglects internal resonances and mooring |
| lightweight torpedo | 0.324 m dia. x 2.6 m long | +6.4 dB BS<br>-22 dB E<br>-15 dB BG | +16 dB BS<br>-22 dB E<br>-15 dB BG | neglects internal resonances and control surfaces |
| heavyweight torpedo | 0.533 m dia. x 5.8 m long | +16 dB BS<br>-18 dB E<br>-9.1 dB BG | +25 dB BS<br>-18 dB E<br>-9.1 dB BG | neglects internal resonances and control surfaces |
| Scuba diver, open system | lungs, tanks, bubble plume | -0.6 dB BS<br>-1.0 dB E<br>-2 dB BG | +3.7 dB BS<br>+10 dB E<br>-2 dB BG | 2 mm bubbles, 5 m plume |
| Scuba diver, rebreather | lungs, tanks only | -6.5 dB BS<br>-8.3 dB E<br>-15 dB BG | +2.3 dB BS<br>+9.5 dB E<br>-15 dB BG | no bubble plume |

Table 1 gives a listing of various targets that might be encountered with a surveillance sonar, with estimates of the *TS* at mid (12 kHz) and high (100 kHz) frequencies. Overall, the *TS* values fall in the range –25 to +10 dB, with some stronger but narrow-angle highlights. These are similar to the ship hull and wake *TS* values found in the following sections, thus the ships serve as useful proxies for these other underwater targets. It has been found that the scattering from fish targets is dominated by the swim-bladder, and some success in modeling fish *TS* using a prolate spheroidal model of the bladder has been successful (e.g. Do and Surti 1990;

Clay and Horne 1994). Similarly the scattering from dolphins and whales has been shown to be dominated by echoes from the lungs (Au 1996). The torpedo models assume a rigid cylinder, although clearly the internal structure will be acoustically penetrable (reducing the highlights). The front-aspect highlight is modeled as a hemispherical cap, and the rear-aspect highlight may be reduced or absent due to the tapered tail and propeller disturbance. For torpedoes the scattering from control surfaces is ignored, but may be important at some aspect angles. A further issue with torpedoes is the potential for generation of a bubbly wake, which occurs for torpedoes with thermal propulsion systems (roughly 50% of currently existing types). The torpedo wake, if present, will further enhance the detectability. The target strength of typical AUVs will be similar to those of the two torpedo types. The scuba diver is assumed to have scattering dominated by two lungs and two air tanks. The lungs are modeled as prolate spheroids with $a$ = semi-minor radius = 0.1 m and $L$ = 0.3 m. The air tanks are modeled as cylinders with $a$ = 0.1 m and $L$ = 0.5 m, with flat bottom end-caps modeled as circular disks and hemispherical top ends. An additional 0.01 $m^2$ cross-section was added to account for all other scattering (e.g. face-mask and dry-suit air layer). The diver's bubble plume was assumed to be 5 m high and modeled using 2 mm diameter non-resonant bubbles produced at a flow rate of 1 litre per second.

## 2. Description of Site and Instrumentation

This sonar monitoring program was conducted within the Drogden shipping channel, which runs roughly north-south between the islands of Amager and Saltholm (see Figure 1) near Copenhagen, DK. Drogden Channel forms an important shipping link between the Baltic Sea to the south and the Øresund to the north, ultimately connecting to the North Sea through the Kattegat. The two sonar installations were installed separately on the western edge of Drogden channel, approximately 200 m northeast of the Nordre-Røse lighthouse. This site was near the narrowest part of the main channel, which at this location was approximately 1 km wide by 11 to 14 m deep. The traffic separation scheme in Drogden Channel had south-bound ships in the western half of the channel (i.e. closest to the sonars) and north-bound ships on the eastern side. There were 500-m-wide shallows (2 to 5 m deep) on either side of this main navigation channel. Tidal heights and currents in this area were small.

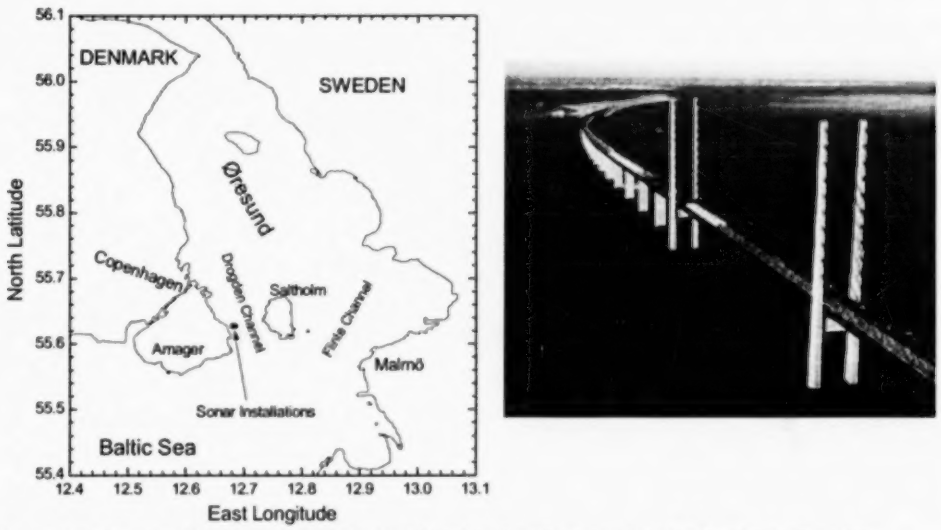


**Figure 1** Left: map of the Øresund and NW Baltic showing the sonar installation site in Drogden Channel. Right: 2002 photograph of new Oresund link bridge looking westward from Malmo towards Drogden Channel, with Amager and Copenhagen in far background.

The 100 kHz sonar was installed in September 1996 on the western edge of Drogden channel, approximately 180 m East of the Nordre-Røse lighthouse. Two 100 kHz sidescan transducers (separate transmit and receive) were mounted on a tripod 1.2 m above the seabed in total water depth of 10.2 m. The sidescan transducers (EDO/Western model 6400) had fan-shaped beams 3° by 60° (total angle to -3 dB). These sonars were mounted with their wide beam axes horizontal and oriented eastward, i.e. perpendicular to the navigation channel. This allowed a wide surveillance area nominally confined to a region within 2 to 5 m above the seabed, with small (<4°) seabed grazing angles. The transducers were attached to a leveling mechanism, operated by divers using a spirit level during the installation. An armored underwater cable connected the sonars to the data acquisition system inside the lighthouse.

The lighthouse station contained a BioSonics Inc. model 101 sonar transceiver, two networked personal computers (PC's), and a radio-modem for telemetering data back to the onshore base station. The sonar receiver provided a 20log[$r$] time-variable gain compensation followed by mix-down to an 8 kHz carrier and amplitude detection. The amplitude-detected signal was then sampled at 1000 samples per second (0.74 m spatial sampling resolution) to a maximum range of 425 m using a PC-based analog to digital converter with 16-bit resolution. A pulse length of 2 ms was used, yielding an acoustic resolution of 1.45 m, transmitted once every 2 s. The data acquisition PC processed the digital data in real time, generating images of backscattered intensity versus range and time, which were then radio-telemetered to shore and printed. The raw data were normally purged a few hours after processing, however during March and April of 1997 most of the raw digital data was stored for later analysis, and this study will focus on this time period. Prior to deployment, the complete 100 kHz sonar system was calibrated utilizing back-scatter from Tungsten-Carbide target spheres as reference (following techniques discussed in Vagle et al. 1996).

The 12 kHz sonar was deployed in October 1997 nearby to the 100 kHz sonar and operated occasionally throughout the winter of 1997/98. This study will focus on data collected during October, 1997. The 2.5 m long array was mounted on a tripod with mechanical steering motor (see Figure 2). It was deployed at 8.4 m depth approximately 200 m northeast of the Nordre-Røse lighthouse, similarly connected by underwater cable. The mechanical steering gear allowed scanning over a 50° sector oriented between North and Northeast across the channel. When in scanning mode the 50° sector was scanned in 2° steps to a range of 2.2 km, providing a measurement area in excess of 2 x $10^6$ $m^2$ once every 150 s. The transceiver and data acquisition system were installed alongside the 100 kHz system inside the lighthouse.

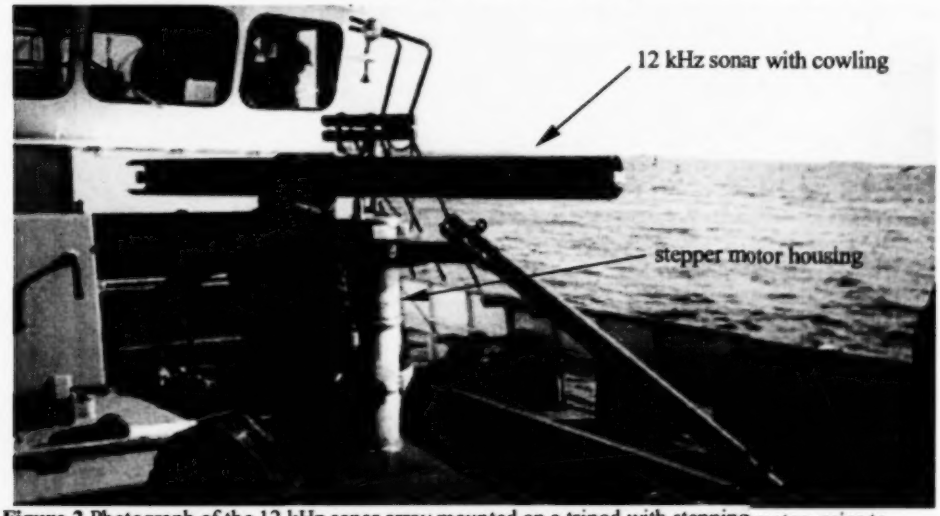


**Figure 2** Photograph of the 12 kHz sonar array mounted on a tripod with stepping motor, prior to deployment in Drogden Channel, Denmark in early October, 1997.

The 12 kHz sonar was a prototype composed of a 40-element (20λ) line array connected to an EDO/Western model 248 Sonar Transceiver. The 12 kHz operating frequency was selected as a compromise between low acoustic absorption and a manageable transducer size while still maintaining directionality. The sonar utilized 40 model TR-229 Tonpilz piston elements

assembled and acoustically calibrated by EDO/Western. The array length was 2.5 m, yielding a one-way horizontal beam width of 2.8° (to -3 dB), with a vertical beam-width of 122° and front-to-back ratio of -6 dB. This front-to-back ratio was improved to approximately -20 dB (one-way) by installing a 30 cm diameter cowling behind the array lined with 12-mm-thick cork-loaded rubber acoustic absorbing material. The transceiver was modified to accept a linear FM sweep from 11.2 to 12.8 kHz of duration up to 50 ms, delivering up to 2.0 kW (electrical) to the array. This provided an on-axis acoustic source amplitude of 63.8 kPa rms. (216 dB re 1 μPa) at 1 m. The received signal was complex heterodyned to a ±1333.3 Hz bandwidth. Complex correlation with the transmit pulse template via FFT processing yielded up to 19 dB processing gain with an effective range resolution of 0.6 m. During this Drogden Channel deployment no time varying gain was used. Calibration of the transceiver and electronic components was carried out in the laboratory at the Institute of Ocean Sciences prior to deployment. Typical pulse repetition intervals were 3.2 s (fixed) and 6.0 s (scanning), with data acquired up to 2200 m range.

For both sonars the calibration results can be used to calculate a scattering level *Equivalent* to *Target Strength* (*ETS*, in dB re 1 $m^2$) at range, $r$, (e.g. Medwin & Clay, 1998)

$$ETS = K + 20 \cdot \log_{10}[A(r)] - TVG(r) + 40 \cdot \log_{10}[r] + 2 \cdot \alpha \cdot r,$$

where $K$ is the calibration coefficient (which includes transmit power, transducer sensitivity, waveform detection, and A/D conversion factors), $A(r)$ is the echo amplitude in digital counts, $TVG(r)$ is the receiver time-varying gain in dB, and $\alpha$ is the acoustic absorption in seawater (0.012 $dB \cdot m^{-1}$ at 100 kHz and 4.1 x $10^{-4}$ $dB \cdot m^{-1}$ at 12 kHz under these water conditions). This equation would yield the *true* backscatter target strength if two factors could be accounted for:

1. correction must be made for the beam deviation loss, i.e. if the target location with respect to the sonar beam was known. For some situations in these field tests the targets can be assumed to lie horizontally along the main beam axis, e.g. at the point of closest approach with a vessel traversing perpendicular to the sonar beam. However, vertical beam pattern corrections are still required, and these require correction for refraction effects.
2. acoustic focusing effects due to propagation (i.e. different from spherical spreading assumed above) can be either calculated or ignored. This requires an acoustic propagation analysis to be performed for the various water conditions found in Drogden Channel. This will be addressed in Section 5.

For environmental monitoring purposes a number of Temperature and Conductivity (TC) sensors and an Acoustic Doppler Current Profiler (ADCP) were deployed in the channel. One of the TC moorings was located approximately 25 m to the east of the 100 kHz sonar, and was visible as a discrete target in all sonar records. This TC mooring had sensors at 5 depths: 2.9, 4.4, 5.6, 7.4, and 9.0 m. The ADCP was bottom mounted at a distance of 135 m from the sonar, and had a similar TC sensor (nominally 10.6 m deep). All sensors were sampled at 30 minute intervals continuously throughout this two-year project. In general the Drogden channel waters were characterized by either a northward flow of relatively fresh (~10 psu) Baltic Sea water or a southward flow of more saline (~20 psu) water from the northern Øresund and the Kattegat. These flow regimes were not dominantly tidal, but driven by wind forcing and seasonal fluctuations.

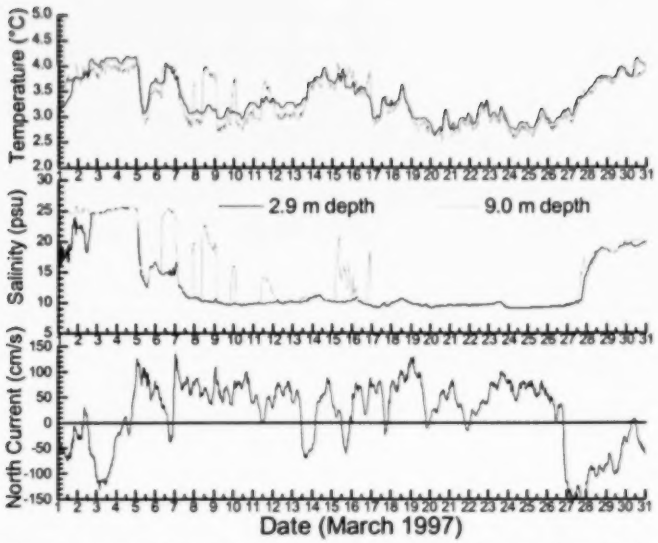


**Figure 3** Comparison of near-surface (2.9 m depth, black) and near-bottom (9 m depth, red) temperature, salinity, and along-channel (North) current at mid-water depth (near 4.8 m depth) in Drogden Channel during March 1997.

Figure 3 presents surface and bottom temperature, salinity, and along-channel (north-south) current data for March, 1997. Although the temperature of both water types was similar (between 2.5°C and 4.5°C during March), the typical salinity of the Kattegat water was 25 psu as compared to the out-flowing Baltic Sea water near 10 psu. Note that diurnal or semi-diurnal tidal signals are only minor perturbations of the along-channel current. Under normal conditions the water was relatively homogeneous in both temperature and salinity. However, during transition periods between the flow regimes, or during very weak Baltic outflows, a vertically stratified flow regime sometimes occurred. These events are clearly evident in Fig. 2 as large differences between surface and bottom salinity, e.g. on March 1$^{st}$, 6$^{th}$, 8$^{th}$, 11$^{th}$, and 15$^{th}$. During March 1997 this stratified flow regime occurred 26% of the time and similar stratified flows were commonly observed throughout the year. The flow in Drogden Channel generally exhibited a vertical profile approximated by a power-law in depth with exponent near 0.25. Thus, the mid-water current magnitude shown in Fig. 3 is 85% of the surface current, with near-bottom (< 1 m above seabed) currents <50% of the surface value.

Figure 4 shows a similar comparison of near-surface and near-bottom temperature, salinity, and sound speed for October, 1997. This time period was characterized by a general cooling trend, from 14° to 8° over the month, but with the waters generally well-mixed in temperature and salinity. Similar to the March period, there were occasional saline intrusions along the bottom that created upward-refracting sound speed profiles. The maximum sound speed difference reached 15 m/s over 6.1 m in depth.

Figure 5 shows the wind speed and direction for the March 1997 period. The average wind speed for this month was 8.7 m/s, significantly above the 5 m/s threshold required for the onset of white-capping and the resultant injection of near-surface bubbles. These bubbles can generate high surface reverberation levels at both sonar operating frequencies. There were

three storm events with wind speeds approaching gale-force. Note that for wind directions with strong westerly or easterly components, which commonly occurred during March, Drogden Channel presents a *fetch-limited* situation. In October, 1997 the winds were generally light, between 4 and 8 m/s for the entire month, creating only minor white-capping conditions.

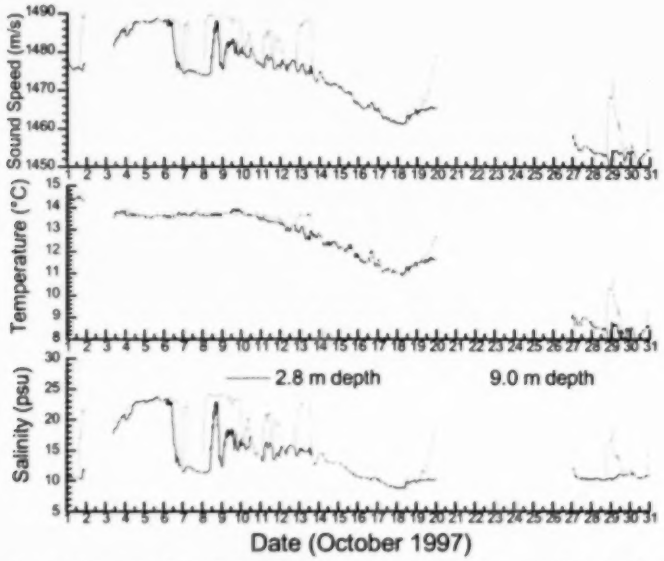


**Figure 4** Comparison of near-surface (2.9 m depth, black) and near-bottom (9 m depth, red) temperature, salinity, and sound speed in Drogden Channel during October 1997.

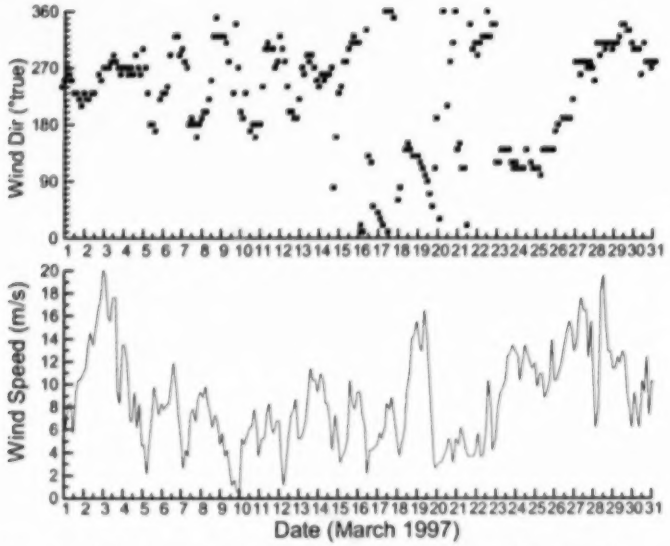


**Figure 5** Wind speed and direction for March 1997 at Drogden Channel, Denmark.

# 3. 100 kHz Reverberation and Target Detection Results

The most common reverberation source for this bottom-mounted sonar was low-grazing-angle seabed backscatter, which provided a relatively time-invariant background against which targets were detected. Figure 6 shows a typical example of relative strength of ship target echoes and the background reverberation under normal flow conditions. Relatively strong seabed backscatter was seen in the range interval 50 to 225 m and beyond 330 m. The figure shows that this seabed reverberation was nearly constant in time, exhibiting distinct lines due to echoes from discrete seabed targets (presumably boulders). The rapid drop in seabed reverberation near 225 m range marked the edge of a roughly 100-m-wide by 3-m-deep gully in the channel bottom. It is also possible that some low levels of sea-surface reverberation contributed at ranges beyond 330 m. The combined reverberation levels beyond 330 m were generally strong enough to mask the ship signatures.

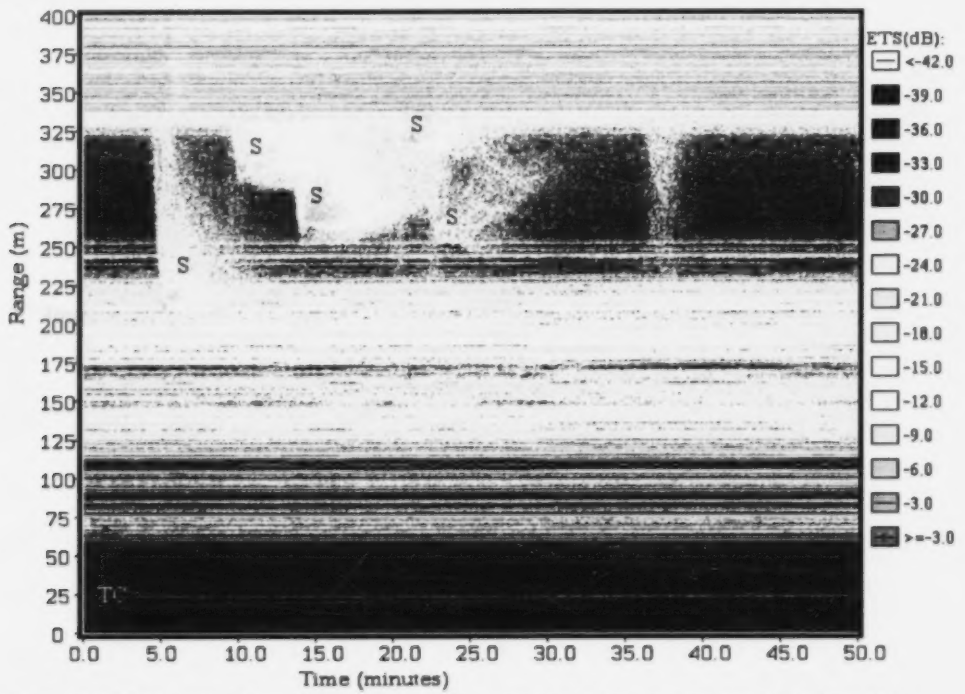


**Figure 6** 100 kHz cross-channel *ETS* (dB re 1 $m^2$) vs. range and time starting 1328UT March 16th, 1997. Labels S indicate ships and TC the echo from temperature-conductivity sensor mooring.

Figure 7 shows a time-averaged profile of this typical 100 kHz reverberation level, calculated during a period without ship targets. Normally, the flow regime was characterized by weakly downward-refracting conditions, so that the sonar (1.2 m above the bottom) insonified the seabed from 20 to 225 m range (the edge of a central gully) and again beyond 330 m range. In the first 225 m the backscatter levels increased rapidly up to approximately -10 dB (re 1 $m^2$) due to the relatively large area of seabed sampled by the 60° horizontal beam aperture. On the far side of the gully the reverberation level reached roughly 0 dB, at times reaching the

A/D clipping level of the sonar. The vertically narrow beam begins to intersect the sea surface at ranges greater than 320 m, allowing low-level sea surface backscatter contributions. The central gully region (225 – 330 m range) lay in an acoustic shadow so that the observed reverberation level dropped to the systemic noise level. On the basis of signal to reverberation ratio, this result shows that large acoustic targets ($TS > 0$ dB) should be detectable with this system at ranges up to 330 m, however smaller targets have the potential to be masked. In the simplest model, the insonified footprint of the sonar on the seabed increases linearly with range, i.e. the variation in $ETS$ with range becomes

$$ETS(r) = S_A(\phi) + 10\log_{10}\left[\tfrac{1}{2}\cdot c\cdot\tau\cdot r\cdot\theta\cdot\cos\phi\right],$$

where $S_A(\phi)$ is the seabed scattering strength (in dB), $c$ is sound speed (1435 m/s), $\tau$ is the pulse length (2 ms), $\phi$ is the seabed grazing angle (< 4°), and $\theta$ is the horizontal beam angle (1.05 radians). The $S_A$ parameter depends on sediment type, frequency, and strongly on grazing angle. Fig. 7 shows a comparison of this simple model using a constant $S_A$ which captures the gross reverberation level at longer range. Closer to the sonar (<150 m) the measured reverberation is lower than the prediction because the backscattered grazing angle along this downward-sloping seabed is very small and seabed returns lie vertically on the edge of the sonar beam. This simple model also assumes that the sediment type and roughness are uniform across the channel. Clearly, a more detailed propagation analysis and beam-pattern correction are necessary to model the seabed backscattering.

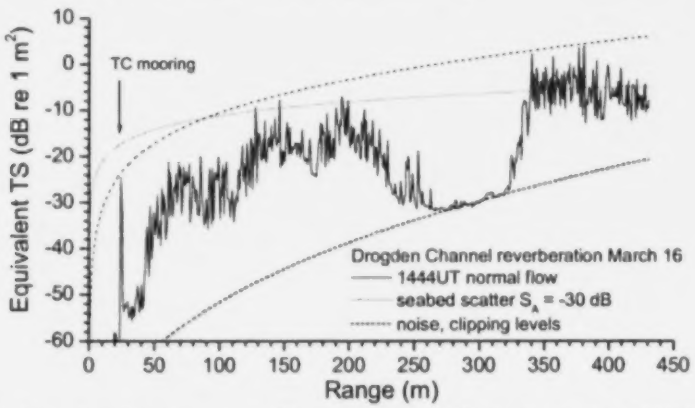


**Figure 7** Seabed reverberation vs. range profile averaged over 20 minutes starting 1444UT, March 16, 1997. Compared to simple seabed scattering model using constant $S_A$ = -30 dB.

Occasional changes in water stratification drastically altered the background reverberation. Figure 8 shows a 100 kHz sonar echogram from a period when the reverberation made a transition from seabed to surface scattering regimes. This transition occurred quite rapidly near 0300UT March 15th, simultaneous with a higher salinity near-bottom intrusion shown in Fig. 3. This salinity stratification created an upward-refracting sound speed gradient of up to 1.8 $s^{-1}$. Prior to the transition the typical seabed backscatter regime was observed, similar to Figs. 6 and 7. Early in the transition the seabed reverberation at ranges >330 m disappeared first. After the transition, the reverberation switched from the seabed regime towards a more homogeneous surface scattering regime. This surface reverberation had a broad maximum roughly 100 m wide, which first appeared at longer range and then moved inwards to 150 m

range as the upward-refracting stratification intensified. The most likely source for this near-surface backscatter was air bubbles injected by white-capping processes.

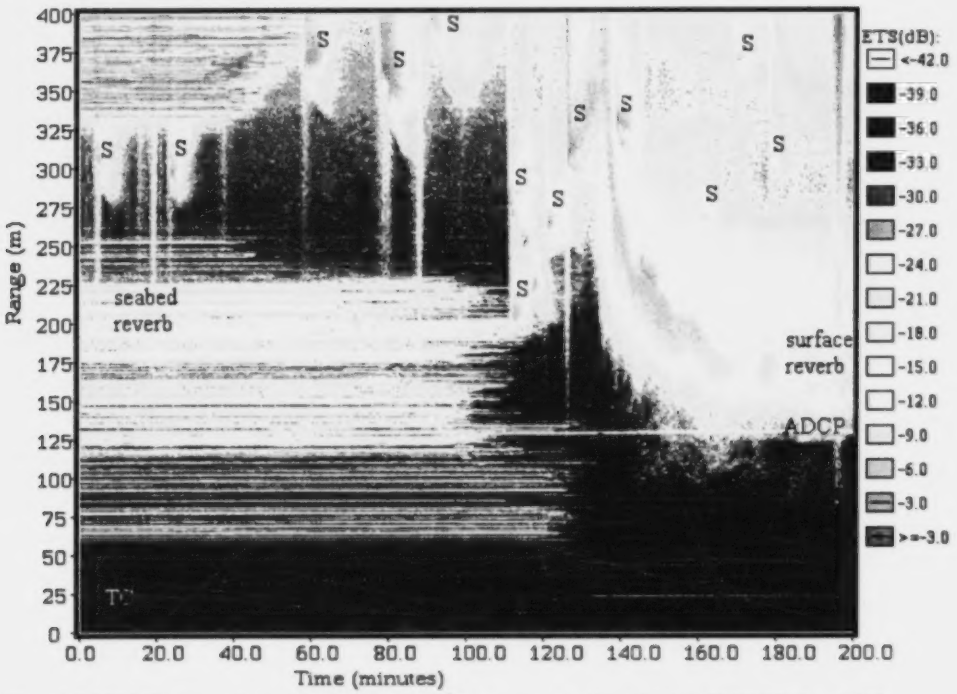


**Figure 8** 100 kHz cross-channel *ETS* (dB re 1 $m^2$) vs. range vs. time starting 0106UT March 15th, 1997. Regions of seabed and surface reverberation are indicated, with labels S indicating ships, TC the echo from temperature-conductivity mooring, and ADCP the echo from a surface float at that location.

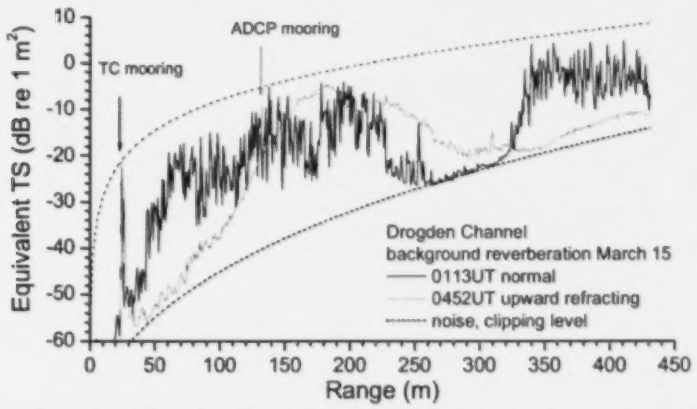


**Figure 9** Comparison of seabed and surface dominated reverberation levels vs. range at 100 kHz, averaged over 10-minute intervals before and after the transition event at 0300UT March 15th, 1997.

Figure 9 compares the seabed and surface reverberation profiles before and after the saline intrusion event shown in Fig. 8. Prior to the transition the seabed reverberation takes on typical values (very similar to Fig. 7). In contrast, the upward-refracting case exhibited a reduced reverberation level at closer range (up to 120 m) due to a minimal interaction with either the surface or seabed. Between 120 and 240 m range the upward-refracting reverberation level increased strongly to a level near -10 dB, similar to the seabed reverberation level, and then reduced beyond 250 m range. In both cases the reverberation curves show a strong peak at 30 m range due to the TC mooring. Finally, note a distinct contrast in *texture* between the two curves, with the seabed reverberation seemingly composed of discrete lines while the surface reverberation was relatively smooth.

In contrast to the effects of stratification, changes in surface wind speed did not have a significant impact on the reverberation under normal flow conditions, as shown in Figure 10. The figure shows the majority of the seabed backscatter structure to be the same with only minor increases in the background noise level within regions where the reverberation normally fell to the systemic noise level, e.g. at $r < 50$ m and 260 m $< r <$ 330 m.

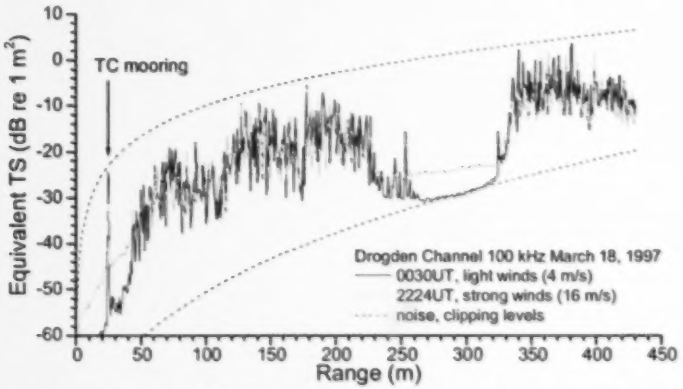
TC mooring
Equivalent TS (dB re 1 m²)
Range (m)
Drogden Channel 100 kHz March 18, 1997
0030UT, light winds (4 m/s)
2224UT, strong winds (16 m/s)
noise, clipping levels

**Figure 10** Comparison of reverberation during periods of light (4 m/s) and strong (16 m/s) surface winds under normal flow conditions, March 18, 1997.

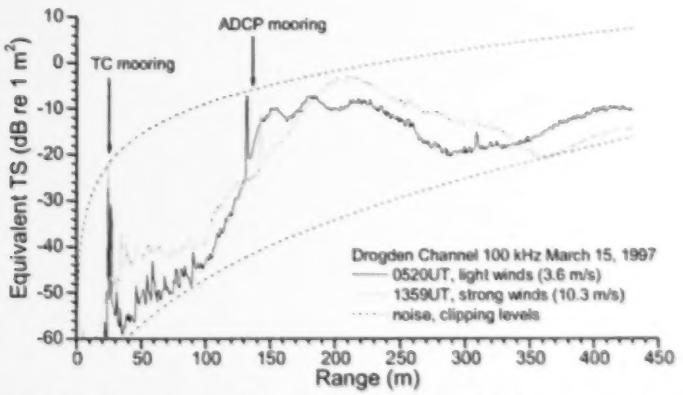
ADCP mooring
TC mooring
Equivalent TS (dB re 1 m²)
Range (m)
Drogden Channel 100 kHz March 15, 1997
0520UT, light winds (3.6 m/s)
1359UT, strong winds (10.3 m/s)
noise, clipping levels

**Figure 11** Comparison of reverberation during periods of light (3.6 m/s) and strong (10.3 m/s) surface winds under saline intrusion flow conditions, March 15, 1997.

The effects of wind for the saline intrusion flow conditions were more subtle. In the example shown in Figure 11, the reverberation profile increased during windy periods by 5 to 10 dB at close range ($r < 120$ m) and in the interval 180 m $< r <$ 340 m. This is due to the increased density and depth-extent of bubbles injected by white-capping processes, which directly increases the backscatter cross-section. A subtle refraction effect was also present, whereby the slightly stronger sound speed gradient in the earlier (light wind) case forced the surface intersection to closer range (170 vs. 210 m). The maximum reverberation for the windy case (near 210 m range) is likely clipped by the A/D converter, but also subject to acoustic extinction effects whereby bubble clouds at closer range absorb and scatter the sonar signal.

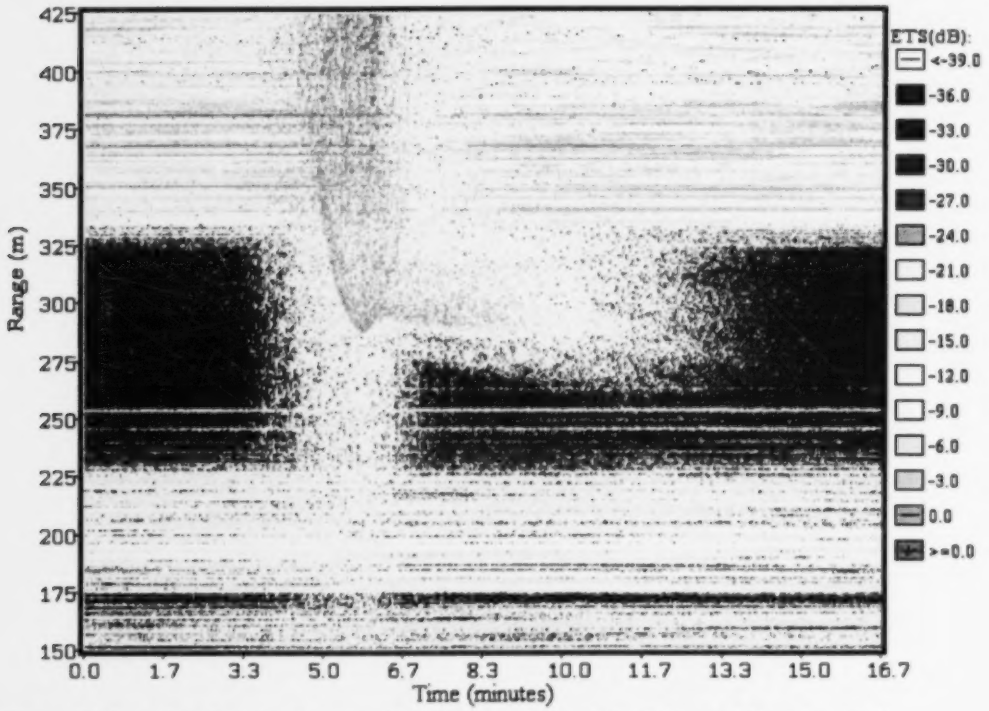


**Figure 12** Example ship wake signature at 0500UT March 22, 1997. Ship speed (from hyperbolic trajectory) was 3.2 m/s with maximum *ETS* (at closest approach) of -0.4 dB (re 1 m$^2$).

An example of a ship signature is detailed in Figure 12. In general, these ship signatures exhibited one or more of the following characteristics:

1. a direct echo from the hull which followed a distinctive hyperbolic trajectory in range vs. time as the ship traversed the horizontally wide beam, i.e. as $r^2 = r_0^2 + u^2(t - t_0)^2$, where $r$ is the range from sonar, $u$ is the vessel speed perpendicular to the sonar axis, and $t$ is time, with $r_0$ and $t_0$ the point of closest approach.
2. an increase in background noise assumed to be caused by propeller cavitation. This noise was accentuated at greater range as a result of the sonar TVG and the conversion to *ETS*. Occasionally, this noise was sufficient to partially mask the ship's hull echo and seabed

reverberation. Infrequently, a regular pulse signature due to the ship's echo-sounder was observed.

3. a strong backscatter region up to 50 m wide following the ship due to the injection of air bubbles within the wake. Frequently these ship wake bubbles masked the seabed reverberation at greater range. These wakes dissipated over a period of 5 to 10 minutes as the bubbles rose to the surface and/or dissolved (see Trevorrow et al. 1994) and/or were advected out of the beam by the current.

Fig. 12 was specifically chosen to show all three characteristics. Many of the ship signatures exhibited only a hull-echo and wake, and some ships only showed a wake. Frequent noise events from northbound ships beyond the maximum sonar range (425 m) were seen. An analysis was made of all the observed ship signatures from March 14 to 31, capturing the characteristics of nearly 660 ships. A hyperbolic functional form was fitted to the observed ship trajectory, allowing estimation of the along-channel ship speed relative to the fixed sonar. This was accomplished through computer-aided visual identification (using a computer mouse) of the target trajectories on range vs. time echograms, although in principle this detection could be done automatically. Also extracted from the ship trajectories were the *ETS* at the point of closest approach, the background reverberation level, and *ETS* of the resulting bubbly wake approximately 30 s after the passage of the vessel.

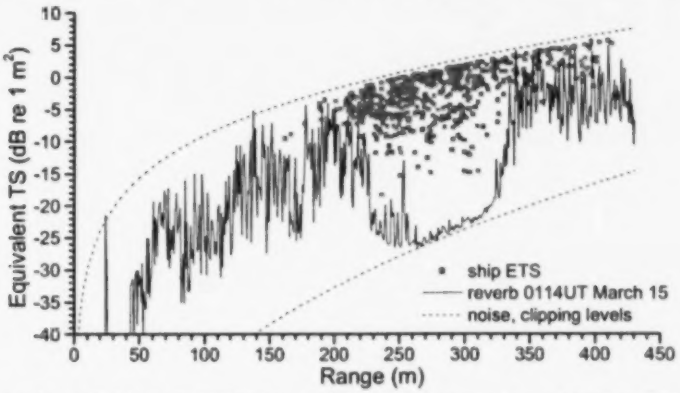


**Figure 13** Comparison of ship hull *ETS* (dB re 1 $m^2$) with background reverberation (0114UT March 15) under normal flow conditions. A total of 593 ship targets were observed from March 14 to 31.

The typical *ETS* of the hull echoes under normal flow conditions is shown in Figure 13. These ETS values, spanning a range of ships from small yachts to freighters and container ships, broadly spanned –19 to 0 dB (re 1 $m^2$), although clearly many of the ship *ETS* were under-estimates as a result of being clipped by the data acquisition system. Overall, the signal to reverberation ratio (SRR) of the detectable ship signatures was broadly distributed from 0 to 20 dB, with a median near 7 dB, although presumably the SRR was also under-estimated due to signal clipping. Note further that correction for vertical beam-pattern and propagation effects have not been made, and for the normal flow conditions both corrections would tend to increase the *ETS* values. The bubbly wakes had a typical maximum *ETS* near –15 to 0 dB, and these wake *ETS* were only loosely correlated with the ship hull *ETS*. Overall, these *ETS* values made ship targets visible up to roughly 400 m range under typical conditions.

The hyperbolic fitting technique produced a very sensitive measure of ship speed. The resultant fit of the hyperbola to the measured trajectory was highly significant (usually with correlation coefficient $r^2 > 0.98$). The distribution of measured ship speeds, shown in Figure 14, spans 2 to 10 m/s. The mean speed (4.8 m/s) is equivalent to roughly 10 knots, which is reasonable for large vessels transiting through a narrow channel. Note that this method alone cannot distinguish the *direction* of ship motion, however the ships' cross-channel range placed them in the south-bound shipping lane. If the sonar beam had been oriented slightly northward or southward, then the ship trajectories would have been skewed, allowing determination of direction of travel.

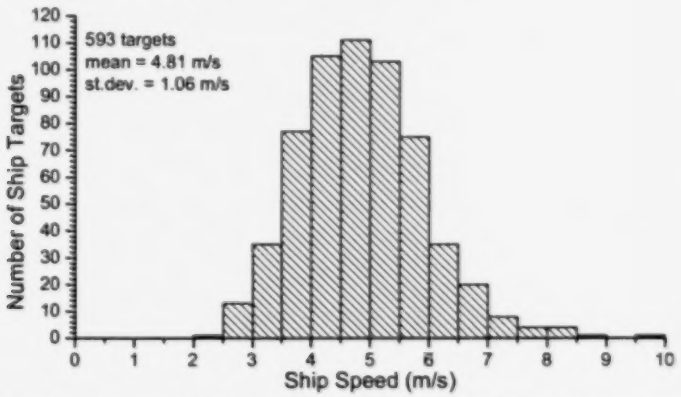


**Figure 14** Distribution of measured ship speeds extracted from hyperbolic trajectory fitting of sonar signatures from March 14-31, 1997 in Drogden Channel.

# 4. 12 kHz Reverberation and Target Detection Results

The 12 kHz sonar was operated for short periods in both fixed-direction and azimuthally-scanning modes. For a half-day period (0500-1838UTC) on 14 October 1997 it was fixed at a heading 020° true, looking roughly 35° away from the channel axis (~345°). During this time-period the flow conditions were normal, i.e. with a relatively unstratified Baltic outflow at roughly 60 cm/s, and the winds were relatively light (3-5 m/s). Data was collected up to 2200 m range using a 20 ms chirp pulse transmitted at 3.125 s intervals, thus covering the entire channel including the north- and south-bound shipping lanes. The geometry of this fixed sonar operation differed from the 100 kHz system in that the sonar beam was much narrower horizontally (2.8° vs. 60°) and the ships were no longer traveling perpendicular to the beam. Also, due to the much lower acoustic absorption and the use of chirp processing, the 12 kHz sonar was able to return echoes from up to 2200 m range in 10-14 m water depth. The echogram in Figure 15 shows typical 12 kHz data, including the signatures of four ships. Similarly to the 100 kHz case, the background seabed reverberation was composed of nominally time-invariant lines, and the ships were identified by their strong signal to reverberation level and transient nature relative to the time-invariant background. Other small cloudlike targets in Fig. 15 are likely fish schools.

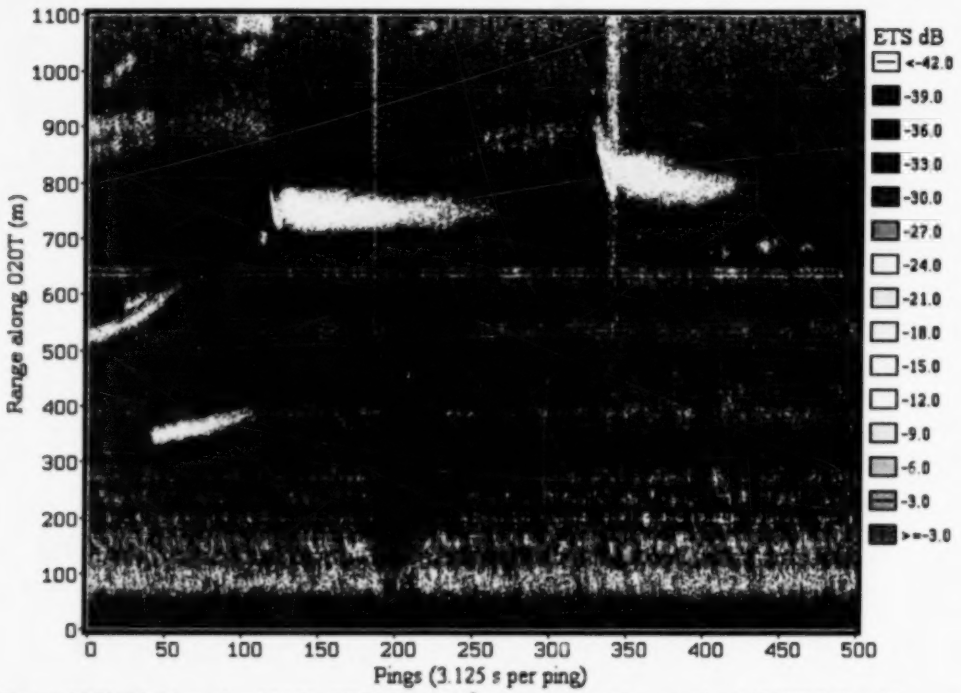


**Figure 15** Fixed orientation 12 kHz *ETS* (dB re 1 $m^2$) vs. range and time starting 1428UTC Oct. 14, 1997 in Drogden Channel.

In this geometry the ships' hull echoes appear as short linear streaks with typical duration of 30 s (about 10 pings). The slope of these streaks is a direct measure of the radial velocity

component, which were typically of magnitude 3 m/s. Radially inwards velocity components were observed in the south-bound shipping lane at 400 – 900 m range, and radially outwards velocities were found in the northbound lane at 1000-1800 m range. The ship signatures generally included a wake, with apparent width up to 80 m and duration of up to 5 minutes. As in the 100 kHz case, the ship signature was often accompanied by a noise line, accentuated at longer range by the *ETS* conversion, and a shadowing of the background reverberation due to acoustic extinction from the wake bubbles. In Fig. 15 the strong dropout at 100-400 m range near ping 190 is likely caused by a ship passing close overhead of the sonar (note the noise line).

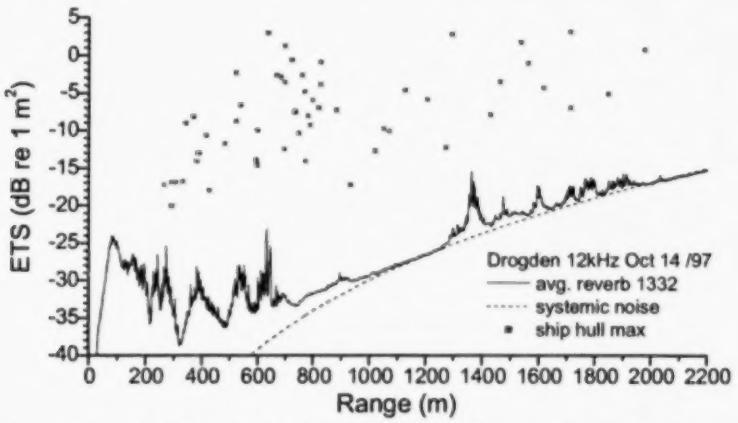


**Figure 16** Comparison of ship's hull *ETS* with background reverberation for the fixed-orientation 12 kHz sonar in Drogden Channel, Oct 14, 1997. Reverberation curve averaged over 1890 pings starting 1332UTC. Ship's hull data taken from 58 ships observed over entire 0500-1838h period.

In general, the background reverberation levels acquired with the 12 kHz sonar were roughly 20 to 30 dB lower than for the 100 kHz, as shown in Figure 16. The maximum reverberation level reached values near –15 dB (re 1 $m^2$) at ranges beyond 1400 m. This is due to a combination of a lower seabed scattering strength at 12 kHz, a much narrower (horizontal) sonar beam and thus insonified area of seabed, and the use of chirp processing. However, the observed *ETS* of the ship hull echoes were similar to the 100 kHz levels, broadly distributed over –20 to +4 dB (re 1 $m^2$). As a consequence, the ship signal-to-reverberation ratio at 12 kHz is much improved, typically reaching 20 to 30 dB, at all ranges up 2000 m. The bubbly ship wake levels were broadly distributed over –30 to –10 dB (re 1 $m^2$), generally about 10 dB lower than the 100 kHz values. However, no definite statement about the relative wake levels can be made without simultaneous measurements on the same wake with the two sonars.

The sector-scanning mode was operated continuously for a 28-hour period starting 1132UTC Oct. 29, 1997. During this period the flow conditions were in transition, changing from a southward, stratified flow to the more normal, unstratified Baltic outflow. The winds were relatively light, dropping from westerly 6 m/s near 1200h on Oct. 29$^{th}$ to variable 3 m/s in the morning of Oct. 30$^{th}$. Data was collected up to 2200 m range using a 50 ms chirp pulse transmitted at 6 s intervals. The additional inter-pulse time was required to mechanically step the sonar in azimuth. The sonar scanned over a 50° sector in 2° steps, thus covering a relatively large sector (2.1 x $10^6$ $m^2$ area) every 150 s. This sector was oriented roughly

northwards along the channel axis, at its maximum range spanning the entire channel, including both the north and south-bound shipping lanes.

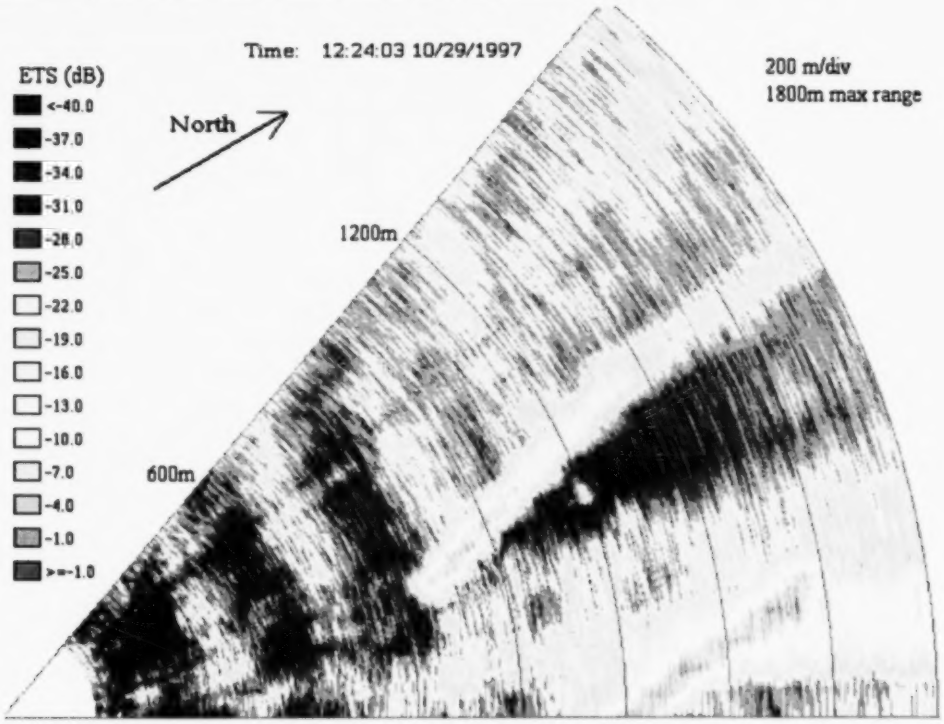


**Figure 17** 12 kHz sector scan image in *ETS* (dB re 1 $m^2$) showing background reverberation and two ship signatures, taken 1224UTC Oct. 29, 1997 in Drogden Channel. Image was constructed from 26 pings covering a 50° by 1800m sector, requiring 150 s to complete.

Figure 17 shows a good example of the sector scan data, in this case with two ships passing roughly 400 m apart. These maps of acoustic scattering allow observation of the speed and direction of ship motion, especially when viewed as *sequences* of images. The only drawback of this sector scanning mode was the relatively slow coverage, such that the ships moved significant distances during the 150 s of the scan. The ship in the bottom right part of the figure near 1600 m range was heading northwards (away from the sonar), and the ship observed in the center of the sector near 850 m range was heading southwards (towards the sonar). The southbound ship wake clearly masked the reverberation behind it (at greater range) by up to 10 dB. The northbound ship exhibited a typical noise line, accentuated at greater range by the *ETS* conversion, as the sonar pointed towards its propeller(s). For comparison, in the fixed-direction mode the sonar was oriented along the bottom edge of this image. The southbound ship trajectory intersects the bottom edge of this sector near 600 m range, in agreement with the southbound ship ranges observed with the sonar in its fixed-orientation (see Fig. 15). At this time the background reverberation exhibited several constant-range bands, approximately 250 m apart, suggestive of upward-refracting conditions, and little azimuthal variability, suggestive that the reverberation was dominated by surface

processes. Later images (e.g. early morning of Oct. 30th) showed generally lower reverberation levels but with more localized azimuthal variations indicative of seabed reverberation features.

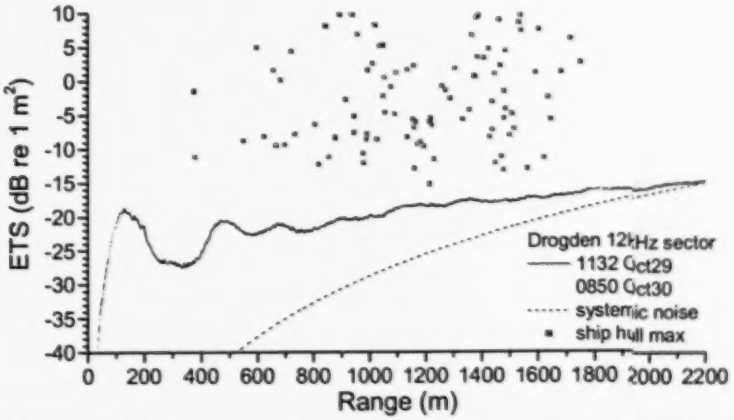


**Figure 18** Comparison of ship's hull *ETS* with background reverberation for the sector scanning 12 kHz sonar in Drogden Channel, Oct 29/30, 1997. Reverberation curves were averaged over 1960 pings at all azimuthal angles. Ship's hull *ETS* taken from 95 ships observed over the entire 28-hour period.

Figure 18 compares the observed ship hull *ETS* with the background reverberation curves at two times during the sector scan tests. The ship hull *ETS* were extracted from the sector images for those instances where the ship trajectory intersected the scanning sonar beam. Some slower ships were hit twice during their transit of the sector, while some faster ships were able to transit the sector while the sonar was *looking the other way*, leaving only a wake. The overall *ETS*, Signal to Reverberation Ratio, and wake *ETS* for the ship targets were similar to those observed in the fixed-orientation mode. The background reverberation did vary during the 28-hours of scanning operation, with Fig. 18 showing the maximum and minimum curves. This is likely due to the combination of two effects: firstly the drop in wind speed from 6 to 3 m/s from 1200 Oct. 29th to 0600 Oct. 30th, and secondly a change in the sound speed profile from upward-refracting to approximately isovelocity over the same time period. The drop in wind speed from above to below the threshold of white-capping is likely responsible for the 5 to 15 dB drop in reverberation levels. Because of the vertically wide sonar aperture the refraction effects are less pronounced than for the 100kHz sonar.

# 5. Propagation Modeling

In this shallow navigation channel the surface and seabed reflections and refraction due to water stratification add important propagation effects that must be included in any quantitative estimates of target strength. The bottom and surface boundaries create a kind of *reflective acoustic waveguide* which generally increases the backscattered amplitude and increases the *effective* pulse length of the echo relative to an unbounded medium. In this particular situation, the use of a relatively long transmitted pulse and the fact that the targets are spatially large implies that the direct and reflected multi-paths to and from a given target are not separable. This complicates the use of echo intensity information for quantitatively estimating the target strength. For both 12 and 100 kHz sonars it is appropriate to model acoustic propagation using ray-tracing. This propagation analysis technique allows determination of the effective insonified volume, the transmission loss to a given region, and the grazing angles at the surface and seabed. A ray-tracing code due to Bowlin et al. (1992) was used to calculate transmission loss as a function of range and depth given the particular sonar geometry, bathymetry, sound speed profiles, and seabed reflection loss.

Figure 19 shows a comparison of the propagation results between the normal and saline intrusion regimes for the 100 kHz sonar. In this analysis, eigenrays connecting the source and a range-depth matrix (10 m range by 0.25 m depth increments) were calculated. The intensity contributions from all multi-paths arriving within 5 ms of the direct path were summed incoherently. For the 100 kHz sonar eigenrays were calculated within a vertical launch angle interval ±3.5° from horizontal, corresponding to the –20 dB points of the transducer beam pattern. The sound speed profiles for the normal and saline intrusion cases were derived from the moored TC data, assuming no range-dependence in water properties. Corrections were made for the transducer beam-pattern, the seawater absorption loss at 100 kHz, a surface reflection loss of 1 dB per bounce, and a seabed reflection loss vs. grazing angle calculated using classical two-layer interfacial theory (e.g. Medwin and Clay, 1998), with a 2 dB loss at angles below critical. The sediments in Drogden Channel were composed of coarse, gravelly sands with assumed density and sound speed of 1900 $kg \cdot m^{-3}$ and 1800 $m \cdot s^{-1}$. This yields a reflection *critical angle* of 37° and a normal-incidence reflection loss of 8.4 dB. Given the near-horizontal sonar beam geometry, all seabed reflections were sub-critical.

Figure 19a shows the ray-tracing calculation for the normal, homogenous flow regime. In this case the vertically-narrow beam is largely confined near the seabed, with a monotonically decreasing normalized Sound Pressure Level (*nSPL*) with range due to acoustic absorption. For this vertically narrow beam at 9.2 m depth, near-surface targets would only be detectable beyond roughly 180 m range (confirmed by a lack of observed ship targets at ranges <150 m in Fig. 13). The typical *nSPL* values in the main beam ranged from –4 to 0 dB, with between 1 and 5 multi-path contributions. This analysis confirms the presence of low-grazing-angle (<3.5°) backscatter from the seabed at ranges from 20 - 225 m and again after 330 m on the far side of the central gully. These ranges of seabed interaction agree with the observed reverberation curve shown in Fig. 7. Additionally, the ray-tracing analysis provides insight on the multi-path structure, for example beyond 50 m range the direct path is supplemented by a low-grazing-angle seabed-reflected path. This seabed-reflected path provides a small increase in *nSPL* that partially counteracts the seawater absorption. Surface-reflected paths exist beyond 180 m range, and are responsible for insonification of the far slope of the central gully near 320 m range.

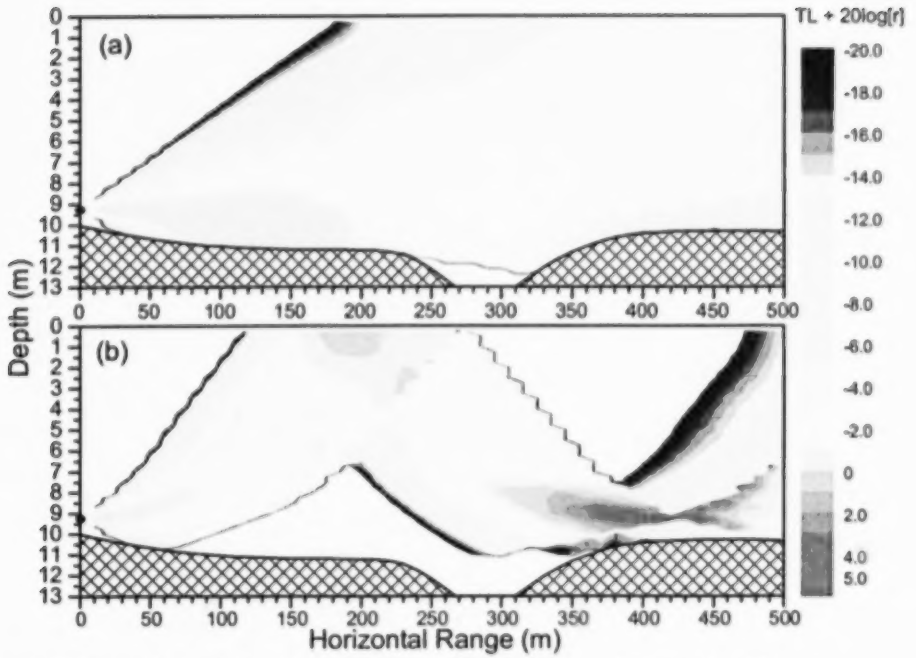


**Figure 19** Comparison of ray-tracing predictions of normalized sound pressure level (one-way transmission loss + 20log[r]) vs. range and depth for the 100 kHz sonar in Drogden Channel. Rays launched ±3.5° from horizontal. (a) normal flow regime. (b) saline intrusion regime.

In contrast, the ray-tracing result for the upward-refracting conditions (Fig. 19b) shows a strong surface reflection and scattering region between 120 m and 280 m, with little seabed interaction beyond 70 m range. Overall there are significant *shadow zones* where targets would be undetectable, making these propagation conditions less suitable for surveillance operations. Within the first near-surface reflection/scattering region at 120 to 270 m range the grazing angle is 4° to 5° and there is a modest acoustic convergence ($nSPL > 0$). In this near-surface focal region the backscatter from air-bubbles would produce significant reverberation. Additionally, near 9 m depth and 350-480 m range there is a very strong ($nSPL > 10$ dB) acoustic convergence region. However this mid-water convergence zone has only a minimal intersection with the seabed, thus generating only a minor contribution to the overall reverberation. Similar to the normal flow case, the propagation analysis is in accordance with the measured upward-refracting reverberation vs. range curve shown in Fig. 7.

The acoustic propagation calculations were repeated for the 12 kHz sonar using seawater conditions that existed in the early afternoons of Oct. 14$^{th}$ (normal, isovelocity flow) and Oct. 29$^{th}$ (upward-refracting). The same eigenray calculations were performed, in this case extending to a range of 2000 m, a depth of 13 m, and calculated within a vertical launch angle interval ±20°. Appropriate values for the acoustic absorption loss at 12 kHz and the transducer beam parameters were used. The bathymetric profile along a heading 020°T (the fixed orientation mode) was extracted from detailed bathymetric charts.

Figure 20 shows a comparison of the propagation results for the 12 kHz sonar. For the normal (isovelocity) case the *nSPL* is approximately depth-independent over the first 1600 m. Within the first 800 m there is a build-up of surface and seabed reflected energy which produces an enhancement in sound pressure level up to +7.1 dB. By 800 m range there are contributions from 18 to 20 significant eigenrays. At greater range the *nSPL* diminishes slightly due to the combined effects of seawater absorption and boundary reflection losses, dropping to roughly +4.5 dB by 2000 m range. Overall, the *nSPL* enhancement and depth-independent insonification make this combination of sonar and water conditions ideal for underwater surveillance.

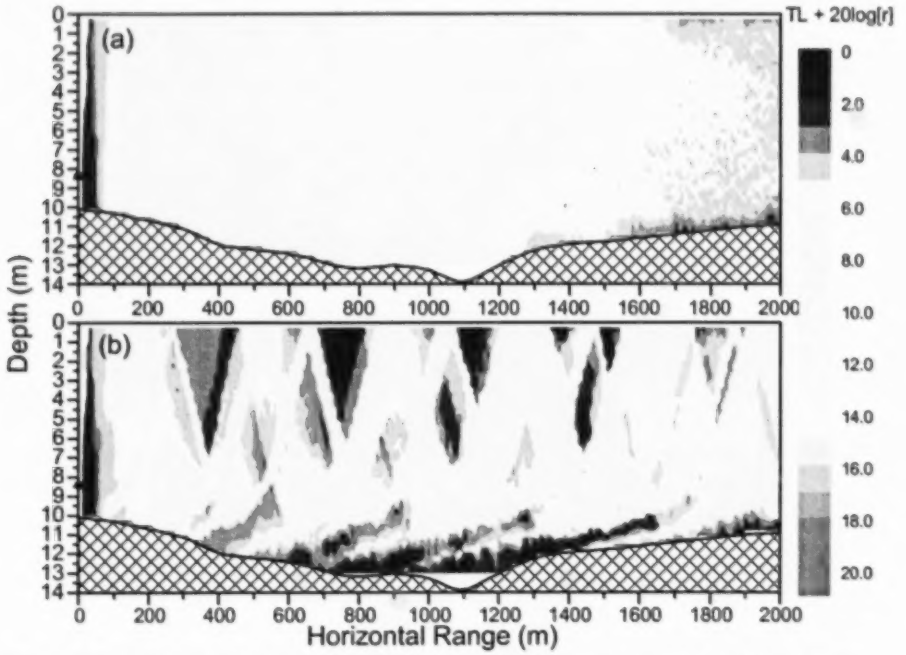


**Figure 20** Comparison of ray-tracing predictions of normalized sound pressure level (one-way transmission loss + 20log[r]) vs. range and depth for the 120 kHz sonar in Drogden Channel. Rays launched ±20° from horizontal. (a) normal flow regime. (b) saline intrusion regime.

In contrast, the saline intrusion regime (Fig. 20b) shows a complicated interference structure, creating convergence and shadow zones that would greatly complicate target detection and tracking. For example, an inbound target at 2 m depth would alternately encounter convergence and shadow regions, potentially being lost and re-acquired multiple times. Upward-refracting ray bundles are reflected multiple times from the surface, producing acoustic convergence zones at the lower turning points near 8.5 m depth. These focal regions can have *nSPL* values reaching 18 to 20 dB. As expected there is limited insonification of the deeper portion of the channel, between 600 and 1200 m range and > 11 m depth. Finally, the locations of the first four surface convergences (near 200, 500, 650, and 900 m range) agree with peaks in the surface-dominated reverberation curve (1132 Oct. 29) shown in Fig. 18.

# 6. Concluding Discussions and Recommendations

Overall, this project demonstrated the feasibility and some characteristics of continuous, active sonar surveillance of a shallow channel. Although these prototype systems were not specially designed for this purpose, they were successful in the detection of ship targets at useful horizontal ranges in this relatively shallow channel. With the 100 kHz sonar ship signatures were observed up to 420 m range with signal to reverberation ratios (SRR) from 0 to 20 dB. With the 12 kHz sonar, ship signatures were detected up to 2000 m away with SRR up to 30 dB. This suggests that a properly designed sonar system could be highly successful for surveillance against AUVs, torpedoes, and divers. Clearly, it was not the goal of this project to monitor surface shipping, as this could be accomplished more easily with radar. However, these surface ships were useful because their *Target Strengths* spanned the expected values for relevant underwater targets such as dolphins, whales, torpedoes, and divers. Moreover, these ship signatures will be a consistent source of interference in any similar sonar surveillance operation, and automatic target detection and tracking algorithms will need to discriminate between ships and other targets.

With both the 12 and 100 kHz sonars it was found that target detectability was strongly limited by boundary reverberation, particularly from the seabed but also on occasion from near-surface bubble layers. In some instances electronic noise was significant, particularly with the 100 kHz sonar at greater range. The importance of seabed reverberation implies that the *location* for any future sonar installation should consider seabed sediment type and bathymetry, favoring low-backscatter muddy, silty, and fine sandy seabeds which are relatively flat. Also, to minimize interference due to surface breaking wave activity exposed and windy sites should be avoided (if possible). In order to identify periods when breaking wave interference will occur, wind speed and direction should be monitored.

The relatively wide horizontal aperture (60°) of 100 kHz sonar made it particularly susceptible to boundary reverberation, with reverberation levels (Equivalent to Target Strength) approaching 0 dB (re 1 $m^2$) at the maximum range. This particular sonar geometry was a compromise between high reverberation levels and the advantages of a wide coverage area, a longer target duration in the beam, and the ability to localize an entire ship (or other target) near the main beam axis. This latter aspect allowed the direct use of echo-amplitude to estimate target strength without the need for a horizontal beam-pattern compensation. In contrast the horizontally narrow-beam 12 kHz sonar had lower reverberation levels, near –15 dB (re 1 $m^2$) at the maximum range (2200 m), but had a much smaller coverage area, particularly in the fixed orientation mode. For the 12 kHz sonar, the ships' duration in the beam was much shorter, typically only a few seconds. The 12 kHz sonar in azimuthally scanning mode provided a very useful 2-dimensional map of the ship target and its wake, however the time required to complete a 25-ping sweep (150 s) was too long and on occasion ships could transit the surveillance sector without detection.

Under normal, relatively homogenous flow conditions ship targets were detectable mostly through their motion relative to the nominally time-invariant seabed reverberation. This occurred even at relatively low SRRs (<10 dB). This leads to the suggestion that examination of the Doppler shift created by moving targets might provide further discrimination against boundary reverberation. However, the reverberation picture was complicated by saline intrusion events which occurred over 10 to 25% of the operating period. These saline intrusions drastically changed the reverberation conditions, creating shadow zones and

rendering target detection through background subtraction more difficult. Clearly, the importance of boundary reverberation and the drastic impact of changing water stratification necessitate the measurement of water properties alongside the sonar installation. These water measurements, when coupled with acoustic propagation analyses, can then be used to predict sonar performance and limitations.

Under normal conditions this shallow water environment acted as a reflective acoustic waveguide. Quantitative ray-tracing calculations showed an increase in the *effective* amplitude of the sonar pulse due to boundary-reflected multi-paths, particularly for the 12 kHz sonar with its vertically wide beam. For example the 12 kHz sonar under normal flow conditions showed one-way propagation enhancements of up to 7 dB in the first 800 m, and this enhancement turned out to be fairly uniform in depth over the entire 2 km operational range. Clearly, this enhancement must be included in quantitative estimates of the Target Strength. However, because the boundary reverberation levels would be similarly enhanced, this effect would only improve target detectability within regions where systemic noise was the dominant limitation. A related issue was the creation of focusing and shadow zones by upward-refracting conditions. For both the 12 and 100 kHz sonars during these saline intrusions there were significant regions where a target could hide, coupled with short-spatial-scale variations in insonification. This has the potential to confound tracking algorithms as the target drops in and out of detectability. The overall conclusion is that the insonified volume is determined largely by the acoustic propagation environment, which can vary with respect to location and on a variety of time scales. Thus it is vital to perform propagation analyses.

Drawing upon the lessons of this study, a general recommendation for an optimal shallow-water surveillance sonar can be proposed:

1. Since the need for longer range detection outweighs the need for high spatial resolution, and that the physical size of the sonar array is generally not critical, a lower frequency sonar operating in the 10 to 50 kHz region would be optimal. The use of FM chirp processing to enhance signal-to-noise properties is advised. Where possible, it is advised to chose an operating frequency outside of the human audible range (i.e. higher than 15 kHz) to avoid noise-pollution issues.
2. The vertical transmit and receive beam-widths should be roughly ±20° (to –3dB), as a compromise between increasing the horizontal directivity and generation/reception of surface and bottom reflected multi-paths.
3. A wide survey aperture, at least 60° but potentially extending to 360° coverage, should be provided. However, the receive beams should be as narrow as practical (of order 1° with minimal side-lobes) to minimize boundary reverberation. It was found that mechanical steering of a single narrow beam was useful but inadequate in terms of sampling speed. Thus, the receiver should be a multi-element array that allows beam-forming into a number of relatively narrow sub-beams. This would allow creation of a 2-dimensional image from a single transmission.
4. Some Doppler shift estimation capability should be provided. This allows separation of targets with non-zero radial velocity from the more stationary (low-Doppler) reverberation.

5. Given the potential for injection of electronic noise within long analog cables, the sonar transmitter, receiver pre-amplifier, and signal digitization electronics should be located close to the sonar transmitter.

It should be noted that many of above recommended features of a surveillance sonar are already available in operational naval hull-mounted sonars (e.g. SQS-510 on Canadian Patrol Frigates). Some modification to the data analysis systems and operator training would likely be necessary for such operations, but this application is entirely within the capabilities of these sonars. This suggests that surveillance of harbours or anchorages could be provided for limited time-periods by operating the hull-mounted sonars while the vessel was anchored or at dockside. The relatively high sonar transmit levels might also serve as a deterrent to SCUBA divers. However, various noise-pollution issues with respect to operating a high-power, audible-frequency (<15 kHz) sonar within a harbour would have to be addressed. Finally, there are several important practical considerations that would greatly favour the use of smaller, seabed-fixed sonar installations:

1. sustaining medium- or long-term (weeks to months) surveillance with a naval vessel is impossible because such vessels have other higher-priority uses.
2. cost: using presently available COTS systems, a useful surveillance sonar could be built and installed for costs ranging from $100k to $500k, with relatively small operational costs thereafter. In contrast, a vessel-mounted sonar is considerably more expensive and the operating costs for maintaining vessel-based operations would be prohibitive.
3. the optimal location for a surveillance sonar may be in shallow water or in close proximity to navigation hazards, rendering positioning of the vessel difficult or impossible.
4. it is difficult to maintain station-keeping over long-periods under adverse weather conditions, whereas sub-surface sonar installations would be relatively immune to surface weather.

One final issue is that active, medium frequency sonars are not covert, and in some applications passive detection may be desirable. In the scenarios imagined for such surveillance sonars, such as monitoring a harbour entrance or a strategic navigation channel such as Drogden, there is no need for covertness. The location of the harbour or channel is usually well-known. In fact, broadcasting the presence of a surveillance system might act as a deterrent. Furthermore, some locations such as harbours are inherently noisy, both from man-made and natural sources, reducing the effectiveness of passive systems. Quiet targets, such as electric-powered AUVs or SCUBA divers, would be difficult to detect in these locations. Finally, it should be noted that some modest level of underwater acoustics expertise would be required to detect sonar transmissions operating above the human audible band (> 15 kHz), making the covert use of active sonars against unsophisticated enemies feasible.

# 7. Bibliography


Au, W., 1996. Acoustic reflectivity of a dolphin, *J. Acoust. Soc. Am.* **99**, 3844-3848.

Boehme, H., Chotiros, N., Rolleigh, L., Pitt, S., Garcia, A., Goldsberry, T., and Lamb, R., 1985. Acoustic backscattering at low grazing angles from the ocean bottom. Part I: Bottom backscattering strength, *J. Acoust. Soc. Am.* **77**(3), 962-974.

Bowlin, J., Spiesberger, J., Duda, T., and Freitag, L., 1992. Ocean acoustical ray-tracing software RAY, Tech. Rep. WHOI-93-10, Woods Hole Oceanographic Institution, Woods Hole, 49pp.

Chapman, D., 1991. Sonar target strength: theoretical considerations, DREA Informal Report UA/91/1.

Clay, C., and Horne, J., 1994. Acoustic models of fish: The Atlantic cod (*Gadus morhua*), *J. Acoust. Soc. Am.* **96**(3), 1661-1668.

Cotaras, F., 1991. Some measurements of target strength at 20-50 kHz, DREA Informal Report UA/90/5.

Do, M., and Surti, A., 1990. Estimation of dorsal aspect target strength of deep-water fish using a simple model of swimbladder back scattering, *J. Acoust. Soc. Am.* **87**(4), 1588-1596.

Dahl, P., and Mathisen, O., 1983. Measurement of fish target strength and associated directivity at high frequency, *J. Acoust. Soc. Am.* **73**, 1205-1211.

Farmer, D., Trevorrow, M., and Pedersen, P., 1999. Intermediate range fish detection with a 12-kHz sidescan sonar, *J. Acoust. Soc. Am.* **106**, 2481-2490.

Francois, R., and Garrison, G., 1982. Sound absorption based on ocean measurements, part II: Boric acid contribution and equation for total absorption. *J. Acoust. Soc. Am.* **72**, 1879-1890.

Love, R., 1973. Target strengths of humpback whales *Megaptera novaeangliae*, *J. Acoust. Soc. Am.* **54**, 1312-1315.

Love, R., 1977. Target strength of an individual fish at any aspect, *J. Acoust. Soc. Am.* **62**, 1397-1403.

Medwin, H., and Clay, C., 1998. Fundamentals of Acoustical Oceanography (Academic Press, San Diego, USA).

McKinney, C., and Anderson, C., 1964. Measurements of backscattering of sound from the ocean bottom, *J. Acoust. Soc. Am.* **36**, 158-163.

Miller, J., and Potter, D., Active high-frequency phased-array sonar for whale shipstrike avoidance: target strength measurements, proceedings MTS/IEEE Oceans 2001, Nov 5-8, 2001 Honolulu, HI., pgs. 2104-2107.

Pedersen, B. and Trevorrow, M., 1999. Continuous monitoring of fish in a shallow channel using a fixed horizontal sonar, *J. Acoust. Soc. Am.* **105**, 3126-3135.

Revie, J., Weston, D., Harden-Jones, F., and Fox, G., 1990. Identification of fish echoes located at 65 km range by shore-based sonar, *J. Cons. Int. Explor. Mer* **46**, 313-324.

Stanton, T. K., 1989. Simple approximate formulas for backscattering of sound by spherical and elongated objects. *J. Acoust. Soc. Am.* **86**(4), 1499-1510.

Trevorrow, M., Vagle, S., and Farmer, D., 1994. Acoustic measurements of microbubbles within ship wakes, *J. Acoust. Soc. Am.* **95**, 1922-1930.

Trevorrow, M., 1997. Detection of migrating salmon in the Fraser River using 100 kHz sidescan sonars, *Can. J. Fish. Aquat. Sci.* **54**, 1619-1629.

Trevorrow, M., 2001. Near-surface environmental limitations to high-frequency sonar performance: a review, Defence Research Establishment Atlantic Tech. Memo. TM2001-002.

Trevorrow, M., 2002. Impacts of flow variability on fixed side-looking 100 kHz sonar performance in a shallow channel, in *Impacts of littoral environmental variability on acoustic predictions and sonar performance*, N. Pace and F. Jensen Eds. (Kluwer Academic Publishers, Dordrecht, the Netherlands).

Vagle, S., Foote, K., Trevorrow, M., and Farmer, D., 1996. Absolute calibrations of monostatic echosounder systems for bubble counting, *IEEE J. Oceanic Eng.* **21**, 298-305.

Weston, D., and Revie, J., 1971. Fish echoes on a long-range sonar display, *J. Sound Vib.* **17**(1), 105-112.

Weston, D., and Revie, J., 1989. A 5-day long-range-sonar record of an extensive concentration of fish, *J. Acoust. Soc. Am.* **86**, 1608-1611.

Weston, D., 1989. On the losses due to storm bubbles in oceanic sound transmission, *J. Acoust. Soc. Am.* **86**(4), 1546-1553.

Wong, H.-K., and Chesterman, W., 1968. Bottom backscattering near grazing incidence in shallow water, *J. Acoust. Soc. Am.* **44**, 1713-1718.

## DOCUMENT CONTROL DATA

(Security classification of title, body of abstract and indexing annotation must be entered when the overall document is classified)

1. ORIGINATOR (the name and address of the organization preparing the document.. Organizations for whom the document was prepared, e.g. Establishment sponsoring a contractor's report, or tasking agency, are entered in section 8.)

Defence Research and Development Canada Atlantic
PO Box 1012
Dartmouth, Nova Scotia, Canada B2Y 3Z7

2. SECURITY CLASSIFICATION (overall security classification of the document including special warning terms if applicable).

UNCLASSIFIED

3. TITLE (the complete document title as indicated on the title page. Its classification should be indicated by the appropriate abbreviation (S,C,R or U) in parentheses after the title).

An evaluation of side-looking 12 and 100 kHz sonars for continuous surveillance of a shallow channel(U)

4. AUTHORS (Last name, first name, middle initial. If military, show rank, e.g. Doe, Maj. John E.)

Trevorrow, Mark V.

| 5. DATE OF PUBLICATION (month and year of publication of document) | 6a. NO .OF PAGES (total containing information Include Annexes, Appendices, etc). | 6b. NO. OF REFS (total cited in document) |
|---|---|---|
| September 2002 | 37 | 27 |

7. DESCRIPTIVE NOTES (the category of the document, e.g. technical report, technical note or memorandum. If appropriate, enter the type of report, e.g. interim, progress, summary, annual or final. Give the inclusive dates when a specific reporting period is covered).

TECHNICAL MEMORANDUM

8. SPONSORING ACTIVITY (the name of the department project office or laboratory sponsoring the research and development. Include address).

Defence Research and Development Canada Atlantic

| 9a. PROJECT OR GRANT NO. (if appropriate, the applicable research and development project or grant number under which the document was written. Please specify whether project or grant). | 9b. CONTRACT NO. (if appropriate, the applicable number under which the document was written). |
|---|---|
| 1DA | |

| 10a ORIGINATOR'S DOCUMENT NUMBER (the official document number by which the document is identified by the originating activity. This number must be unique to this document.) | 10b OTHER DOCUMENT NOs. (Any other numbers which may be assigned this document either by the originator or by the sponsor.) |
|---|---|
| DRDC-Atlantic TM 2002-149 | |

11. DOCUMENT AVAILABILITY (any limitations on further dissemination of the document, other than those imposed by security classification)

( ✔ ) Unlimited distribution
( ) Defence departments and defence contractors; further distribution only as approved
( ) Defence departments and Canadian defence contractors; further distribution only as approved
( ) Government departments and agencies; further distribution only as approved
( ) Defence departments; further distribution only as approved
( ) Other (please specify):

12. DOCUMENT ANNOUNCEMENT (any limitation to the bibliographic announcement of this document. This will normally correspond to the Document Availability (11). However, where further distribution (beyond the audience specified in (11) is possible, a wider announcement audience may be selected).



DCD03 2/06/87-M/ DREA mod. 17 Dec 1997

13. ABSTRACT (a brief and factual summary of the document. It may also appear elsewhere in the body of the document itself. It is highly desirable that the abstract of classified documents be unclassified. Each paragraph of the abstract shall begin with an indication of the security classification of the information in the paragraph (unless the document itself is unclassified) represented as (S), (C), (R), or (U). It is not necessary to include here abstracts in both official languages unless the text is bilingual).

(U) This study evaluates data from two high-frequency (12 and 100 kHz) side-looking sonars which were operated for extended periods in March and October 1997 in Drogden Channel, near Copenhagen, Denmark. This busy shipping channel, 1-km-wide by 12-m-deep, connects the Baltic Sea with the North Sea through the Kattegat. The original purpose of these tests was to demonstrate continuous surveillance for migratory herring, however a variety of shipping traffic was also observed. Quantitative acoustic measurements of ship characteristics and low-grazing-angle seabed reverberation were made with both sonars under a variety of conditions. The sonar measurements were supplemented by simultaneous water temperature, salinity, and current profiles and surface meteorological measurements, allowing some understanding of the environmental influences. The general characteristics were that under normal, homogeneous flow conditions, ships and fish schools were routinely observed up to 400 m range with the 100 kHz sonar and up to 2000 m range with the 12 kHz system. Occasional saline intrusions near the seabed were observed to create strong upward-refracting conditions that significantly altered the available range for target detection, especially for the 100 kHz sonar. Example echograms and reverberation results from both normal and upward-refracting conditions are shown. Ray-tracing analysis is used to assess the acoustic propagation conditions, specifically to define insonified volumes and shadow zones, and quantify the reflection focusing effects.

14. KEYWORDS, DESCRIPTORS or IDENTIFIERS (technically meaningful terms or short phrases that characterize a document and could be helpful in cataloguing the document. They should be selected so that no security classification is required. Identifiers, such as equipment model designation, trade name, military project code name, geographic location may also be included. If possible keywords should be selected from a published thesaurus. e.g. Thesaurus of Engineering and Scientific Terms (TEST) and that thesaurus-identified. If it not possible to select indexing terms which are Unclassified, the classification of each should be indicated as with the title).

sidescan sonar, boundary reverberation, target strength, ray-tracing analysis, surveillance

**Defence R&D Canada**

**Canada's leader in defence and national security R&D**

**R & D pour la défense Canada**

**Chef de file au Canada en R & D pour la défense et la sécurité nationale**

**www.drdc-rddc.gc.ca**